https://doi.org/10.5194/bg-2020-410
Preprint. Discussion started: 13 November 2020

Biogeosciences Discussions

Global geographic variability in freshwater methane hydrogen isotope ratios and its implications for emissions source apportionment and microbial biogeochemistry

Peter M.J. Douglas[1], Emerald Stratigopoulos[1], Jenny Park[1], Dawson Phan[1]

[1]Earth and Planetary Sciences, McGill University, Montreal, H3A 0E8, Canada

Correspondence to: Peter M. J. Douglas (peter.douglas@mcgill.ca)

Abstract. There is growing interest in developing spatially resolved methane (CH_4) isotopic source signatures to aid in geographic source attribution of CH_4 emissions. CH_4 hydrogen isotope measurements (δ^2H-CH_4) have the potential to be a powerful tool for spatial resolution of CH_4 emissions from freshwater environments, as well as other microbial sources. This is because microbial δ^2H-CH_4 values are partially dependent on the δ^2H of environmental water (δ^2H-H_2O), which exhibits large and well-characterized spatial variability globally. We compiled a comprehensive global dataset of paired CH_4 δ^2H and $\delta^{13}C$ measurements from freshwater environments, including wetlands, inland waters, and rice paddies, comprising a total of 131 different ecosystems, and compared these with measurements and estimates of δ^2H-H_2O. We found that the estimated δ^2H of annual precipitation (δ^2H_p) explained approximately 35% of the observed variation in δ^2H-CH_4, and that the relationship between δ^2H-CH_4 and δ^2H_p led to significant differences in the distribution of freshwater δ^2H-CH_4 between the northern high latitudes (60-90 ºN) relative to other global regions. Residual variability in δ^2H-CH_4 is partially explained by differences in the dominant methanogenic pathway and CH_4 oxidation, as inferred from carbon isotope fractionation between CH_4 and carbon dioxide (α_C). Our results imply that hydrogenotrophic methanogenesis is characterized by a steeper slope of δ^2H-CH_4 vs. δ^2H_p than acetoclastic methanogenesis, a pattern that is consistent with previous predictions. Biogeochemical sources of variability in δ^2H-CH_4 are reflected in apparent differences between different freshwater ecosystems, with relatively high values in rivers and bogs, and low values in fens and rice paddies, although more data is needed to verify whether these differences are significant. To estimate how changes in the spatial distribution of freshwater emissions would influence global atmospheric CH_4 isotopic measurements, we developed a 'bottom-up' mixing model of global CH_4 δ^2H and $\delta^{13}C$ sources, including spatially resolved signatures for freshwater CH_4 sources. This model implies that changes in high-latitude freshwater CH_4 emissions would have an especially strong influence on global source δ^2H-CH_4. We estimate that global CH_4 emissions sources have a combined δ^2H value of -277±8‰, which is consistent with 'top-down' estimates based on atmospheric measurements. In contrast our estimated $\delta^{13}C$ value of -56.4±1.4‰ is not consistent with atmospheric measurements, suggesting possible errors in either emissions inventories or estimates of sink fluxes and isotopic fractionations. Overall our results emphasize the value of δ^2H-CH_4 measurements to help constrain atmospheric CH_4 budgets.

https://doi.org/10.5194/bg-2020-410
Preprint. Discussion started: 13 November 2020

1 Introduction

Methane (CH_4) is an important greenhouse gas that accounts for approximately 25% of current anthropogenic global warming, but we do not have a complete understanding of the current relative or absolute fluxes of different CH_4 sources to the atmosphere (Saunois et al., 2020; Schwietzke et al., 2016), nor is there consensus on the causes of recent decadal-scale changes in the rate of increase in atmospheric CH_4 (Turner et al., 2019; Pison et al., 2013; Schaefer et al., 2016; Kai et al., 2011; Rice et al., 2016). Freshwater ecosystems are an integral component of the global CH_4 budget. They are one of the largest sources of atmospheric CH_4 and are clearly the largest natural, or non-anthropogenic, source (Saunois et al., 2020; Bastviken et al., 2011). At the same time the geographic distribution of freshwater CH_4 emissions, changes in the strength of this source through time, and the relative importance of wetland versus inland water CH_4 emissions all remain highly uncertain (Saunois et al., 2020; Turner et al., 2019; Ganesan et al., 2018; Pison et al., 2013; Schaefer et al., 2016). Gaining a better understanding of freshwater CH_4 emissions on a global scale is of great importance for understanding potential future climate feedbacks related to CH_4 emissions from these ecosystems (Koven et al., 2011; Yvon-Durocher et al., 2014; Zhang et al., 2017; Bastviken et al., 2011). It is also necessary in order to better constrain the quantity and rate of change of other CH_4 emissions sources, including anthropogenic sources from fossil fuels, agriculture, and waste (Kai et al., 2011; Pison et al., 2013; Schaefer et al., 2016).

Isotopic tracers, particularly $\delta^{13}C$, have proven to be very useful in constraining global CH_4 sources and sinks (Schwietzke et al., 2016; Kai et al., 2011; Rice et al., 2016; Schaefer et al., 2016). However, $\delta^{13}C$ source signatures cannot fully differentiate CH_4 sources, leaving residual ambiguity in source apportionment (Turner et al., 2019; Schaefer et al., 2016). Applying additional isotopic tracers to atmospheric CH_4 monitoring has the potential to greatly improve our understanding of CH_4 sources and sinks (Turner et al., 2019; Saunois et al., 2019). In particular, recent technological developments have the potential to make atmospheric δ^2H-CH_4 measurements more practical at higher spatial and temporal resolution (Yacovitch et al., 2020; Chen et al., 2016; Röckmann et al., 2016; Townsend-Small et al., 2016). δ^2H-CH_4 measurements have proven useful in understanding past CH_4 sources in ice-core records (Bock et al., 2010; Whiticar and Schaefer, 2007; Bock et al., 2017; Mischler et al., 2009), but have seen only limited use in modern atmospheric CH_4 budgets (Rice et al., 2016; Kai et al., 2011), in part because of loosely constrained source terms, as well as relatively sparse atmospheric measurements.

δ^2H-CH_4 measurements could prove especially useful in understanding freshwater CH_4 emissions. Freshwater δ^2H-CH_4 is thought to be highly dependent on δ^2H-H_2O (Waldron et al., 1999b; Chanton et al., 2006; Whiticar, 1999). Since δ^2H-H_2O exhibits large geographic variation as a function of temperature and fractional precipitation (Bowen and Revenaugh, 2003; Rozanski et al., 1993), δ^2H-CH_4 measurements have the potential to differentiate freshwater CH_4 sources by latitude. This approach has been applied in some ice core studies (Bock et al., 2010; Whiticar and Schaefer, 2007), but geographic source signals remain poorly constrained, in part because of small datasets and because of incompletely understood

https://doi.org/10.5194/bg-2020-410
Preprint. Discussion started: 13 November 2020


Biogeosciences Discussions Open Access EGU

relationships between δ^2H-H_2O and δ^2H-CH_4. In contrast, recent studies of modern atmospheric CH_4 δ^2H have not accounted for geographic variation in freshwater CH_4 sources (Rice et al., 2016; Kai et al., 2011).

Freshwater δ^2H-CH_4 is also thought to vary as a function of biogeochemical variables, including the biochemical pathway of methanogenesis and the extent of CH_4 oxidation (Whiticar, 1999; Chanton et al., 2006). These influences on δ^2H-CH_4 have the potential to complicate geographic signals, but also provide the potential to differentiate ecosystem sources if specific ecosystems are characterized by differing methanogenic pathways and rates of CH_4 oxidation. A recent study proposed that freshwater δ^{13}C-CH_4 could be differentiated geographically based on ecosystem differences in methanogenic pathways and carbon sources, in addition to the geographic distribution of wetland ecosystems (Ganesan et al., 2018). δ^2H-CH_4 measurements have the potential to complement this approach by providing an additional isotopic parameter for defining ecosystem and geographic CH_4 source signatures.

In order to use δ^2H-CH_4 as an indicator of freshwater ecosystem contributions to global and regional CH_4 emissions budgets, a clearer understanding of freshwater δ^2H source signals, and how they vary by geographic location, ecosystem type, and other variables is needed. In order to address this need we have assembled and analyzed a dataset of 967 δ^2H-CH_4 measurements from 131 individual ecosystems, or sites, derived from 38 publications (Alstad and Whiticar, 2011; Bellisario et al., 1999; Bergamaschi, 1997; Bouchard et al., 2015; Brosius et al., 2012; Burke and Sackett, 1986; Burke et al., 1988, 1992; Burke, 1992; Cadieux et al., 2016; Chanton et al., 1997; Chanton et al., 2006; Chasar et al., 2000; Douglas et al., 2016; Happell et al., 1993; Happell et al., 1994; Hornibrook et al., 1997; Lansdown, 1994; Lansdown et al., 1992; Lecher et al., 2017; Levin et al., 1993; Marik et al., 2002; Martens et al., 1992; Nakagawa et al., 2002a; Nakagawa et al., 2002b; Popp et al., 1999; Sakagami et al., 2012; Schoell, 1983; Stolper et al., 2015; Thompson et al., 2016; Tyler et al., 1997; Wahlen, 1994; Waldron et al., 1999a; Walter et al., 2006; Walter et al., 2008; Wang et al., 2015; Wassmann et al., 1992; Whiticar et al., 1986; Woltemate et al., 1984; Zimov et al., 1997). While previous studies have assembled datasets of freshwater δ^2H-CH_4 (Waldron et al., 1999b; Sherwood et al., 2017; Whiticar et al., 1986), this dataset represents an advance relative to those studies in four key attributes: 1) it is significantly larger than previous datasets, with 83 additional sites relative to Waldron et al., (1999); 2) paired δ^{13}C-CH4 data is available for all sites, δ^{13}C-CO_2 data is available for 50% of sites, and δ^2H-H_2O data is available for 47% of sites; 3) all sites are geo-located, providing the potential to perform spatial analyses and compare with gridded isotopic datasets of precipitation isotopic composition; and 4) we classify all sites by ecosystem and sample type (dissolved vs. gas samples), allowing for a clearer differentiation of how these variables influence δ^2H-CH_4.

Using this data set we then applied statistical analyses to address key questions surrounding the global distribution of freshwater δ^2H-CH_4, the variables that control this distribution, and its potential implications for atmospheric δ^2H-CH_4. Specifically, we investigated the nature of the global dependence of δ^2H-CH_4 on δ^2H-H_2O, and whether this relationship results in significant differences in freshwater δ^2H-CH_4 by latitude. We also assessed whether variability in methanogenic pathways and methane oxidation, as inferred from δ^{13}C-CH_4, δ^{13}C-CO_2, and α_C, induce significant variability in δ^2H-CH_4, and whether this resulted in significant differences in δ^2H-CH_4 between different ecosystem and sample types. Finally, we

https://doi.org/10.5194/bg-2020-410
Preprint. Discussion started: 13 November 2020

used our dataset, combined with other isotopic datasets (Sherwood et al., 2017) and flux estimates (Saunois et al., 2020), to estimate the global δ^2H-CH_4 and δ^{13}C-CH_4 of global emissions sources, compared this with estimates based on atmospheric measurements (Rice et al., 2016), and assessed the sensitivity of atmospheric δ^2H-CH_4 to differences in the latitudinal distribution of freshwater emissions.

2 Methods

2.1 Isotope Nomenclature

We use a wide range of isotope notation in this study, which is briefly introduced here. Hydrogen and carbon isotope ratios are primarily discussed as delta values, using the generalized formula:

$$\delta = \frac{\left(R_{\text{sample}} - R_{\text{standard}}\right)}{R_{\text{standard}}} \quad (1)$$

Where R is the ratio of the heavy isotope to the light isotope, and the standard is Vienna Standard Mean Ocean Water (VSMOW) for δ^2H and Vienna Pee Dee Belemnite (VPDB) for δ^{13}C. δ values are expressed in per mil (‰) notation.

We also refer to the isotopic fractionation factor between two phases, or α, which is defined as:

$$\alpha_{a-b} = \frac{R_a}{R_b} = \frac{\delta_a + 1000}{\delta_b + 1000} \quad (2)$$

Specifically, we discuss carbon isotope fractionation between CO_2 and CH_4 (α_C) and hydrogen isotope fractionation between H_2O and CH_4 (α_H).

For δ^2H-H_2O we differentiate between measured water samples (δ^2H-H_2O_m) and the modelled isotopic composition of annual precipitation at a given location (δ^2H_p), as is discussed further in Sect. 2.2.3. To account for the effects of δ^2H-H_2O on δ^2H-CH_4, we introduce the term δ^2H-$CH_{4,W0}$, which is the estimated δ^2H-CH_4 of a sample if it had formed in an environment where δ^2H-H_2O = 0‰. This is defined by the equation:

$$\delta^2\text{H-CH}_{4,\text{W0}} = \delta^2\text{H-CH}_4 - \left(b \times \delta^2\text{H}_p\right) \quad (3)$$

Where *b* is the slope of the regression relationship of δ^2H_p vs. δ^2H-CH_4 for the entire dataset, as reported in Sect. 3.3. We use this value instead of α_H because, as discussed in Sect. 3.4, the global relationship between δ^2H_p vs. δ^2H-CH_4 does not correspond to a constant value of α_H, and therefore deviations from this empirical relationship are more clearly expressed as a residual as opposed to a fractionation factor.

https://doi.org/10.5194/bg-2020-410
Preprint. Discussion started: 13 November 2020

123 **2.2 Dataset Compilation**

124 **2.2.1 Literature Survey**

125 To identify datasets we used a set of search terms (methane OR CH_4 AND freshwater OR wetland OR peatland OR swamp
126 OR marsh OR lake OR pond OR 'inland water' AND 'hydrogen isotope' OR 'δD' OR 'δ^2H' in Google Scholar to find
127 published papers that discussed this measurement. We also identified original publications using previously compiled
128 datasets (Sherwood et al., 2017; Waldron et al., 1999b). Data for 90% of sites were from peer-reviewed publications. Data
129 from 13 sites were from a masters thesis (Lansdown, 1994).

130 **2.2.2 Dataset structure**

131 Most samples were associated with geographic coordinates in data tables or text documentation, or with specific geographic
132 locations such as the name of a town or city. In a few cases we identified approximate geographic locations based on text
133 descriptions of sampling sites, with the aid of Google Earth software. Sampling sites were defined as individual water bodies
134 or wetlands as identified in the relevant study. In some cases where a number of small ponds were sampled from the same
135 location we grouped ponds of a given type as a single site (Bouchard et al., 2015). We divided sampling sites into five
136 ecosystem categories: lakes and ponds (hereafter lakes), rivers and floodplains (hereafter rivers), bogs, fens, swamps and
137 marshes, and rice paddies. Swamps and marshes were combined as one category because of a small number of sites, and
138 because there is no clear indication of biogeochemical differences between these ecosystems. To make these categorizations
139 we relied on site descriptions in the data source publications. We also analyzed data in two larger environment types, inland
140 waters (lakes and rivers) and wetlands (bogs, fens, swamps and marshes, and rice paddies). While rice paddies are an
141 anthropogenic ecosystem, they are wetlands where microbial methanogenesis occurs under generally similar conditions to
142 natural wetlands, and therefore we included them in our analysis. In some cases the type of wetland was not specified. We
143 did not differentiate between ombrotrophic and minerotrophic peatlands since most publications did not specify this
144 difference, although it has been inferred to be important for $\delta^{13}C$-CH_4 distributions (Hornibrook, 2009).
145 We also categorized samples by the form in which CH_4 was sampled, differentiating between dissolved CH_4 and
146 CH_4 emitted through diffusive fluxes, which we group as dissolved CH_4, and gas-phase samples, including bubbles sampled
147 either by disturbing sediments or by collecting natural ebullition fluxes. In some cases the sampling method or type of
148 sample was not specified, or samples were a mix of both categories, which we did not attempt to differentiate.
149 Where possible (78% of sites), δ^2H-CH_4 and $\delta^{13}C$-CH_4 values, as well as $\delta^{13}C$-CO_2 and δ^2H-H_2O, were gathered
150 from data files or published tables. In a number of publications, representing 22% of sites, data were only available
151 graphically. For these studies we used Webplot Digitizer (https://automeris.io/WebPlotDigitizer/) software to extract data for
152 these parameters. Previous studies have shown that user errors from Webplot Digitizer are typically small (Drevon et al.,
153 2017). Studies where data was derived from graphs are identified in Supplementary Table S1 (Douglas et al., 2020).

https://doi.org/10.5194/bg-2020-410
Preprint. Discussion started: 13 November 2020

154 **2.2.3 Estimated Isotopic Composition of Precipitation**

155 To compare δ^2H-CH_4 and δ^2H-H_2O measurements with estimates of δ^2H_p, we used the Online Isotopes in Precipitation
156 Calculator v.3.1 (OIPC; www.waterisotopes.org; (Bowen and Revenaugh, 2003;Bowen and Wilkinson, 2002;Bowen et al.,
157 2005). Inputs for δ^2H_p estimates are latitude, longitude, and elevation. We estimated elevation for each site surface elevation
158 at the site's geographic coordinates reported by Google Earth. We tabulated estimates of annual precipitation δ^2H_p, under the
159 assumption that this is generally the best estimate of freshwater ecosystem δ^2H (See Sect. 3.2).

160 **2.3 Statistical analyses**

161 **2.3.1 Site level mean values and uncertainties**

162 For all statistical analyses we use site-level mean isotopic values. This avoids biasing our analyses towards sites with large
163 numbers of measurements. There are large differences in the number of samples analyzed per site (*n* ranges from 66 to 1).
164 To generalize uncertainty in δ^2H-CH_4 across different studies, we calculated a pooled standard deviation for all studies with
165 multiple measurements, following a modification of the methods recommended by Polissar and D'Andrea (2013) for
166 molecular δ^2H measurements, using the following equation:

167 $$SD_{pooled} = \sqrt{\frac{(n_1-1)s_1^2 + (n_2-1)s_2^2 + \ldots + (n_k-1)s_k^2}{n_1+n_2+\ldots n_k - k}} \quad (4)$$

168 Where *n* is the number of samples measured per site, s is the site-level standard deviation, and k is the total number
169 of sites with multiple sample measurements. We then estimated the standard error of the mean for each site, including sites
170 with only one measurement, using the following calculation:

171 $$SE_{pooled} = \frac{SD_{pooled}}{\sqrt{n}} \quad (5)$$

172 **2.3.2 Regression analyses**

173 We perform a set of simple and multiple linear regression analyses CH_4 δ^2H against other isotopic variables, in
174 addition to latitude. All statistical analyses were performed in Matlab. We performed weighted regression to account for
175 differences in uncertainty between sites, with weighting equal to $1/SE_{pooled}$. For regression analyses we considered a
176 relationship to be statistically significant when the $p < 0.05$.

177 δ^2H-CH_4 is predicted to be a non-linear function of δ^{13}C-CH_4, δ^{13}C-CO_2, and α_C. This is because variation in
178 methanogenic pathway is predicted to result in negative co-variation between δ^2H-CH_4 and δ^{13}C-CH_4, and positive co-
179 variation between δ^2H-CH_4 and δ^{13}C-CO_2 and α_C. Conversely, methane oxidation is predicted to result in positive co-

https://doi.org/10.5194/bg-2020-410
Preprint. Discussion started: 13 November 2020


Biogeosciences Discussions Open Access EGU

variation between δ^2H-CH_4 and δ^{13}C-CH_4, and negative co-variation between δ^2H-CH_4 and δ^{13}C-CO_2 and α_C (Chanton et al., 2006; Whiticar, 1999). To test for this non-linear co-variation we applied a piece-wise linear regression approach (Bailer, 2020), with the goal of identifying at what value for the independent variable the linear relationship between the two variables changed. We used the Shape Language Modeling package in Matlab to perform this analysis. We compared our results with predicted co-variation between these variables based on isotopic fractionation factors and empirical classification of isotopic signatures presented by Whiticar (1999), as shown in Supplementary Table S2 (Douglas et al., 2020). Specifically, predictions of δ^{13}C-CH_4, δ^{13}C-CO_2, and α_C are derived from Figure 8 in Whiticar (1999), and predictions of δ^2H-$CH_{4,W0}$ are derived from Figures 5 and 10 in Whiticar (1999). These figures are used widely to interpret environmental isotopic data related to CH_4 cycling.

2.3.3 Sample set comparison tests

To compare isotopic data (δ^2H-CH_4 and δ^{13}C-CH_4) between groups (i.e. latitudinal bands, ecosystem types, sample types) we used non-parametric statistical tests to test whether the groups were from different distributions. We used non-parametric tests because some sample groups were not normally distributed, as determined by a Shapiro-Wilk test (Shapiro and Wilk, 1965). For comparing the distributions of two groups we used the Mann-Whitney U-test (Mann and Whitney, 1947), whereas when comparing more than two groups we used the Kruskal-Wallis H-test (Kruskal and Wallis, 1952), combined with Dunn's test to compare specific sample group pairs (Dunn, 1964). We considered $p < 0.05$ to be the threshold for identifying groups with significantly different distributions.

2.4 Estimation of global atmospheric CH_4 δ^2H and δ^{13}C source values

To better understand how latitudinal differences in wetland isotopic source signatures influence atmospheric δ^2H-CH_4 and δ^{13}C-CH_4, we calculated a 'bottom-up' mixing model of δ^2H-CH_4 and δ^{13}C-CH_4. For this calculation we ascribed all CH_4 sources a flux and δ2H and δ^{13}C value, and calculated the global atmospheric source value using an isotopic mixing model. Because of non-linearity when mixing δ^2H values, we performed the mixing equation using isotopic ratios (see Sect. 2.1). The mixing equation is as follows:

$$R_{mix} = f_1 R_1 + f_2 R_2 + \ldots + f_n R_n \quad (6)$$

Where f_n is the fractional flux for each source term (i.e. the ratio of the source flux to total flux), and R_n is the isotope ratio for each source term.

Values for the flux, δ^2H, and δ^{13}C applied for each source term are shown in Table 1. We used bottom-up source fluxes from Saunois et al. (2020) for the period 2008-2017. Because other natural sources are not differentiated for the

https://doi.org/10.5194/bg-2020-410
Preprint. Discussion started: 13 November 2020

period 2008-2017, we calculated the proportional contribution of each category of other natural sources for the period 2000-2009 (Saunois et al., 2020), and applied this to the total flux from other natural sources for 2008-2017. For categories other than wetlands, inland waters, and rice paddies, we used global fluxes and δ^2H values, since geographically resolved δ^2H estimates are not available. For these sources we used δ^2H values published by Sherwood et al. (2017), using the mean value for each source term. For wetlands, inland waters, and rice paddies, we used geographically resolved (60-90 ºN; 30-60 ºN, 90º S-30ºN) fluxes derived from Saunois et al. (2019) for the period 2008-2017, and mean δ^2H for these latitudinal bands from this study. Inland waters and rice paddies do not have geographically resolved fluxes reported in Saunois et al. (2019). Therefore, we calculated the proportion of *other natural sources* attributed to inland waters from 2000-2009 (71%), and applied this proportion to the geographically resolved fluxes of *other natural sources*. Similarly, we calculated the proportion of *agricultural and waste sources* that attributed to rice agriculture from 2008-2017 (15%), and applied this to the geographically resolved fluxes of *agricultural and waste fluxes*.

To estimate uncertainty in the modelled total source δ^2H and $\delta^{13}C$ values we conducted Monte Carlo analyses (Thompson et al., 1992). We first estimated the uncertainty for each flux, δ^2H, and $\delta^{13}C$ term. Flux uncertainties were defined as one half of the range of estimates provided by Saunois et al., (2020). For sources where fluxes were calculated as a proportion of a larger flux, we applied the same proportional approach to estimate uncertainties. In cases where one half of the range of reported studies was larger than the flux estimate, we set the uncertainty to be equal to the flux estimate to avoid negative fluxes in the mixing model. Isotopic source signal uncertainties were defined as the 95% confidence interval of the mean value for a given source category. For some sources there is insufficient data to calculate a 95% confidence interval, and we applied a conservative estimate of uncertainty for these sources, as detailed in Table 1. We then recalculated the δ^2H and $\delta^{13}C$ mixing models 10,000 times, each time sampling inputs from the uncertainty distribution for each variable. We assumed all uncertainties were normally distributed. We interpret the standard deviation of the resulting Monte Carlo distributions as an estimate of the uncertainty of our total atmospheric CH_4 source isotopic values. To examine how the Monte Carlo analyses were specifically influenced by uncertainty in isotopic source signatures versus flux estimates, we conducted sensitivity tests where we set the uncertainty in either isotopic source signatures or flux estimates to zero.

To estimate the sensitivity of atmospheric CH_4 isotopic measurements to changes in freshwater fluxes by latitude we calculated the incremental change in the total atmospheric source δ^2H-CH_4 and $\delta^{13}C$-CH_4 under idealized scenarios of increasing freshwater emissions from the low-latitudes, mid-latitudes, and high-latitudes up to an increase of 40 Tg/yr, with all other emissions sources remaining constant. 40 Tg/yr was chosen since it is within the range of estimates of the possible CH_4 emissions feedbacks to global warming from both high-latitude and low-latitude freshwater environments (Koven et al., 2011; Zhang et al., 2017). We performed a similar analysis for total fossil fuel and biomass burning emissions. Finally, we compared these predicted patterns of isotopic variation with estimates of changes in global source δ^2H-CH_4 and $\delta^{13}C$-CH_4 between 1977 and 2005 based on atmospheric CH_4 isotopic measurements combined with estimates of sink fluxes and

https://doi.org/10.5194/bg-2020-410
Preprint. Discussion started: 13 November 2020

242 isotopic fractionations (Rice et al., 2016). We refer to the estimates of global source signatures from Rice et al., (2016) as
243 'top-down' estimates, in contrast to our 'bottom-up' estimates of global source δ^2H-CH_4 and δ^{13}C-CH_4.
244

Table 1: Estimates of source-specific fluxes, δ^2H-CH4, and δ^{13}C-CH4, and their uncertainties, used in mixing models and Monte Carlo analyses

	Flux		δ^2H signature		δ^{13}C signature	
Category	(Tg/Yr)	Uncertainty	(‰, VSMOW)	Uncertainty	(‰, VPDB)	Uncertainty
Wetlands (<30N)	115	37.5	-301	15	-64.9	1.7
Wetlands (30-60N)	25	16.5	-319	14	-62.6	2.5
Wetlands (>60N)	9	8.0	-373	10	-61.8	2.5
Inland Waters (<30N)	80	39.4	-293	24	-56.4	4.8
Inland Waters (30-60N)	64	31.9	-308	18	-61.6	5.3
Inland Waters (>60N)	16	7.5	-347	9	-65.0	2.2
Geological (onshore)[a]	38	13.0	-189	44	-43.8	10.0
Wild animals[b]	2	2.0	-316	28	-65.4	3.5
Termites[c]	9	6.0	-343	50	-63.4	3.5
Permafrost soils (direct)[d]	1	0.5	-373	15	-64.2	1.7
Geological (offshore)[a]	7	7.0	-189	44	-43.8	10.0
Biogenic open and coastal[e]	6	3.0	-200	50	-80.0	20.0
Enteric fermentation and manure	111	5.0	-308	28	-65.4	3.5
Landfills and waste	65	4.5	-297	6	-56.0	4.9
Rice cultivation (<30N)	19	1.2	-324	8	-54.0	4.9
Rice cultivation (30-60N)	12	0.5	-325	8	-59.1	4.9
Coal mining	42	15.5	-232	5	-49.5	1.0
Oil and gas	79	13.0	-189	2	-43.8	0.5
Industry[f]	3	3.0	-189	2	-43.8	0.5
Transport[f]	4	4.0	-189	2	-43.8	0.5
Biomass burning[g]	17	6.0	-211	15	-26.2	2.0
Biofuel burning[g]	12	2.0	-211	15	-26.2	2.0

a-No specific isotopic measurements in database. We applied the mean isotopic values for oil and gas, and applied the standard deviation of these values as the uncertainty
b-No specific isotopic measurements in database. We used the isotopic values and uncertainties from livestock
c-Only one δ^2H measurement in database. We applied 50‰ as a conservative uncertainty estimate.
d- No specific isotopic measurement in database. We used the isotopic values and uncertainties for high-latitude wetlands
e- No specific isotopic measurements in database. We applied approximate isotopic values based on Whiticar, (1999), and conservatively large uncertainty estimates.
f-No specific isotopic measurements in database. We used the isotopic values and uncertainties for oil and gas.
g-We applied all isotopic measurements of biomass burning to both the biomass burning and biofuel burning categories

https://doi.org/10.5194/bg-2020-410
Preprint. Discussion started: 13 November 2020

3 Results

3.1 Dataset distribution

The dataset is primarily concentrated in the northern hemisphere (Fig. 1A), but is distributed across a wide range of latitudes between 3 ºS to 73 ºN (Figure 1B). The majority of sampled sites are from North America, but there are numerous sites from Eurasia (Fig. 1A). A much smaller number of sites are from South America and Africa. We define three latitudinal bands for describing geographic trends: low latitudes (3 ºS to 30 ºN); mid-latitudes (30 ºto 60 ºN); and high-latitudes; (60º to 90º N). This definition was used primarily because it corresponds with a commonly applied geographic classification of CH_4 fluxes (Saunois et al., 2020).

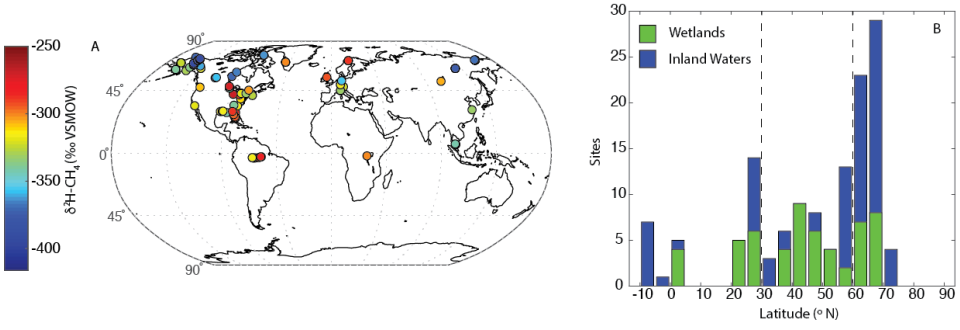

Figure 1: Global distribution of data shown; A) on a world map, with site mean CH_4-δ^2H values indicated in relation to a color bar; and B) as a histogram of sites by latitude, differentiated between wetlands and inland waters. Dashed lines in (B) indicate divisions between low-latitude, mid-latitude, and high-latitude sites.

76 of 131 sites are classified as inland waters, primarily lakes (n = 67), with a smaller number from rivers (n = 9). To our knowledge, all of the inland water sites are natural ecosystems and do not include reservoirs. 55 sites are classified as wetlands, including 16 bogs, 14 swamps and marshes, 12 fens, and 8 rice paddies. For the majority of sites (n =84) gas samples were measured, whereas studies at 36 sites measured dissolved CH_4 or diffusive fluxes.

3.2 Use of δ^2H_p as an estimator for freshwater δ^2H-H_2O

As discussed in Sect. 2.2.3, we estimated δ^2H-H_2O using modelled precipitation δ^2H_p. Identifying the relationship between modelled δ^2H_p and δ^2H-CH_4 is of value because global distributions of δ^2H_p are routinely estimated using isotope enabled Earth system models (Zhu et al., 2017), and could potentially be used to predict the distribution of δ^2H-CH_4 under past and future global climates. In addition, this approach allows us to examine co-variation of δ^2H-CH_4 and δ^2H-H_2O at sites where δ^2H-H_2O was not measured. However, modelled annual δ^2H_p is not a perfect estimator of δ^2H-H_2O in freshwater environments. Comparing modelled δ^2H_p with measured δ^2H-H_2O for 62 sites indicates generally good agreement at low and high values of δ^2H_p, but also that δ^2H-H_2O is generally higher than predicted at intermediate values of δ^2H_p (Fig. 2). We infer

https://doi.org/10.5194/bg-2020-410
Preprint. Discussion started: 13 November 2020

that this is because in our dataset wetlands are concentrated in the mid-latitudes (Fig. 1B), and because wetlands could be more likely to experience changes in δ^2H-H_2O on a seasonal basis because of overall smaller water volumes than lakes (Clay et al., 2004). However, the root mean square error (RMSE) for the 1:1 line (23‰) is not substantially larger than the RMSE for the best-fit linear relationship shown in Fig. 2 (19‰). Based on this, and on the rationale for analyzing δ^2H-CH_4 in terms of δ^2H_p as described above, we proceed with this analysis. However, we also examine how the relationship between δ^2H_p vs. δ^2H-CH_4 differs from that for δ^2H-H_2O_m vs. δ^2H-CH_4 (Sect. 3.3).

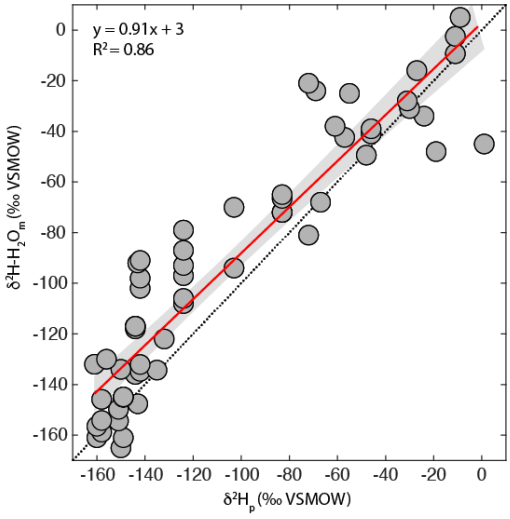

Figure 2: Scatter plot of δ^2H-H_2O_m vs. δ^2H_p for 62 sites with δ^2H-H_2O measurements. The red line indicates the best fit, with a 95% confidence interval (gray envelope), and the dashed black line is a 1:1 relationship.

3.3 Relationship between δ^2H-H_2O and δ^2H-CH_4

δ^2H-CH_4 is significantly positively correlated with both δ^2H_p and δ^2H-H_2O_m (Fig. 3a). The slope of δ^2H-CH_4 vs. δ^2H-H_2O_m (0.45±0.18) is steeper than that for δ^2H-CH_4 vs. δ^2H_p (0.38±0.09), but the two regression slopes have overlapping confidence intervals across their entire range. Given the regression parameters, and the similar RMSE for these two relationships (33‰ vs. 29‰), we infer that using δ^2H_p to predict δ^2H-CH_4 does not result in substantial error. Both relationships result in a large amount of unexplained residual variability, implying the importance of other variables in controlling δ^2H-CH_4. Both slopes are flatter than the regression relationship found by Waldron et al. (1999b) using a smaller dataset (0.68±0.1). The regression relationship of Waldron et al. (1999b) overlaps with the confidence intervals of our results at more positive values of δ^2H-H_2O (>~60‰), but implies more negative values of δ^2H-CH_4 when δ^2H-H_2O is lower. The intercepts of all three regression relationships are within error of one another.

https://doi.org/10.5194/bg-2020-410
Preprint. Discussion started: 13 November 2020

Biogeosciences Discussions Open Access EGU

When the data are disaggregated by environment type, we observe significant positive relationships between δ^2H_p vs. $\delta^2H\text{-}CH_4$ for both wetlands and inland waters (Fig. 3b). The regression equation for wetlands has a steeper slope (0.56±13) than that for inland waters (0.32±.12). The confidence intervals for these regression equations are clearly different for low values of δ^2H_p, below about -120‰. The wetland relationship is closer to, but still flatter than, that of Waldron et al. (1999b).

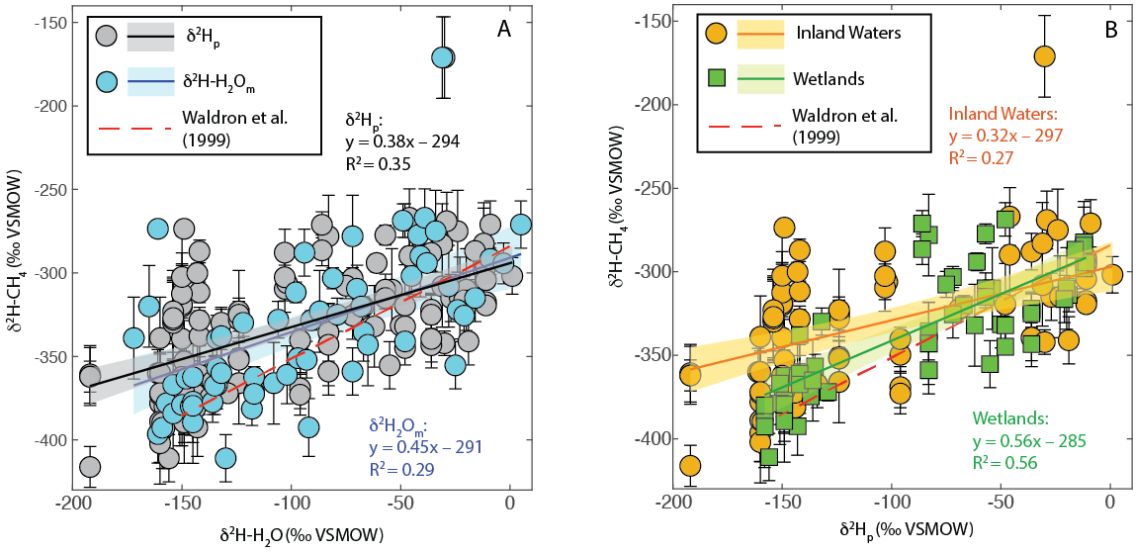

Figure 3: (A) Scatter plot of $\delta^2H\text{-}CH_4$ vs. both $\delta^2H\text{-}H_2O_m$ and δ^2H_p for all data. (B) Scatter plot of $\delta^2H\text{-}CH_4$ vs. δ^2H_p with data disaggregated by environment type. Envelopes indicate 95% confidence intervals for regression lines. The relationship of Waldron et al., (1999) is indicated by a red dashed line. Error bars indicate pooled standard error for $\delta^2H\text{-}CH_4$ as described in Sect. 2.3.1.

Given that δ^2H_p is strongly influenced by latitude, although it is also influenced by other geographic and climatic variables, we examined whether $\delta^2H\text{-}CH_4$ is also significantly correlated with latitude. There is indeed a significant, but weak negative relationship between latitude and $\delta^2H\text{-}CH_4$, indicating an approximate decrease of 0.9‰/ ° latitude (Fig. 4). The slope is significantly flatter than that for latitude vs. δ^2H_p in this dataset (-2.3 ‰/ ° latitude), which is consistent with the relatively flat slope for δ^2H_p vs. $\delta^2H\text{-}CH_4$.

https://doi.org/10.5194/bg-2020-410
Preprint. Discussion started: 13 November 2020

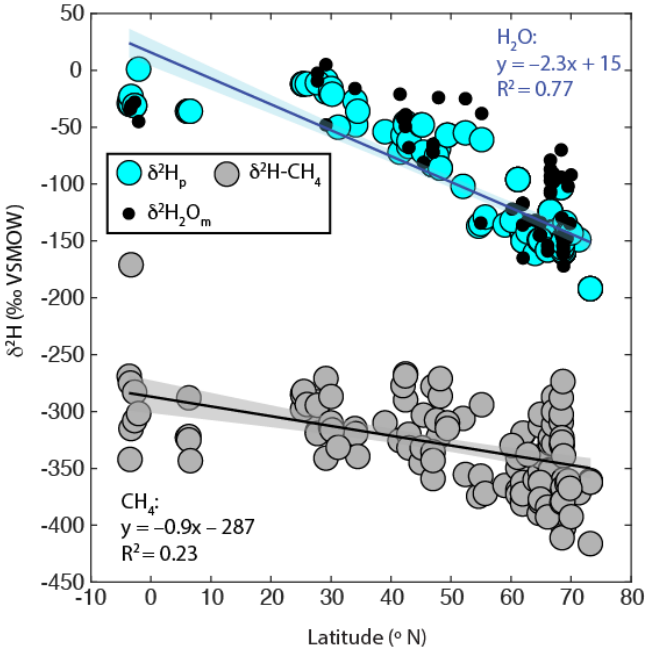

Figure 4: Scatter plots of δ^2H-CH_4, δ^2H-H_2O_m, and δ^2H_p vs. latitude. Envelopes indicate 95% confidence intervals for regression lines.

3.4 Relationship of δ^2H-CH_4 with δ^{13}C-CH_4, δ^{13}C-CO_2, and α_C

We do not find evidence for a piece-wise linear relationship between δ^{13}C-CH_4 and δ^2H-$CH_{4,W0}$ (Fig. 5a), nor did we find a significant simple linear correlation between these variables. This is true both for the dataset as a whole, and for the subset of sites with δ^{13}C-CO_2 values, which we analyzed for the sake of comparability. In contrast we did find evidence for a piece-wise linear relationships between δ^2H-$CH_{4,W0}$ and both α_C and δ^{13}C-CO_2 that is broadly consistent with predictions (Fig. 5b,c). This analysis suggests that the breakpoint, or the point at which variation in δ^2H-$CH_{4,W0}$ shifts from being controlled by variation in methanogenesis pathway to being controlled by CH_4 oxidation, is approximately $\alpha_C = 1.036$ and δ^{13}C-$CO_2 = -16$‰. α_C is a better predictor of variation in δ^2H-$CH_{4,W0}$ overall, and especially for variation related to CH_4 oxidation, for which we do not observe a significant linear relationship with δ^{13}C-CO_2. We also observe similar piece-wise linear relationships between these two variables and raw δ^2H-CH_4 values, although the R^2 values are for the most part lower.

Based on the results shown in Fig. 5b, we classified samples into three categories based on α_C values: oxidation influenced ($\alpha_C < 1.036$); dominantly fermentation ($1.036 < \alpha_C < 1.055$); and dominantly hydrogenotrophy ($\alpha_C \geq 1.055$). The definition of oxidation-influenced samples is based on the breakpoint discussed above. The division between the dominantly

https://doi.org/10.5194/bg-2020-410
Preprint. Discussion started: 13 November 2020

Biogeosciences Discussions Open Access EGU

fermentation and dominantly hydrogenotrophy categories is based on the median α_C value, excluding sites where CH_4 oxidation is inferred. We note that an α_C value of 1.055 corresponds to previous divisions between methanogenesis pathways (Whiticar, 1999).

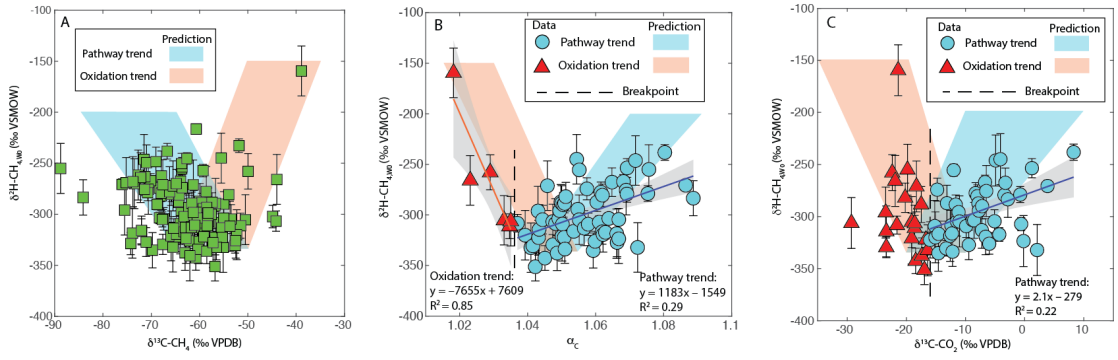

Figure 5: Scatter plots of δ^2H-$CH_{4,w0}$ vs. (A) δ^{13}C-CH_4, (B) α_c, and (C) δ^{13}C-CO_2. Predicted variation for variation in methanogenic pathway and CH_4 oxidation are shown by colored parallelograms, with details on predicted values in Supplementary Table 2 (Douglas et al., 2020). Significant ($p < 0.05$) piece-wise regression relationships are shown in (B) and (C), with breakpoints shown by dashed lines. No significant relationships were observed in (A). Grey envelopes indicate 95% confidence intervals for regression lines. Error bars indicate pooled standard error for δ^2H-CH_4.

We then performed linear regression analyses between δ^2H-CH_4 and δ^2H_p within these two groups to examine whether methanogenic pathway influenced this relationship (Fig. 6). For the high α_C category (dominantly hydrogenotrophy) there is a positive correlation with a relatively steep slope (0.68±0.18). This regression line is within error of the line predicted by an α_H of 1.35 (Fig. 6). In contrast, for the intermediate α_C group (dominantly fermentation) the slope is lower (0.39±0.13), similar to that for the dataset as a whole. This relationship does not agree consistently with a constant value of α_H. The confidence intervals for these two regression relationships do not overlap for values of δ^2H_p greater than -110‰. If sites where oxidation is inferred are excluded, a multivariate linear regression analysis finds a significant dependence of δ^2H-CH_4 on both δ^2H_p and α_C (adjusted $R^2 = 0.67$; RMSE = 22‰). The multivariate regression equation is:

$$\delta^2\text{H-CH}_4 = 0.52\delta^2H_p + 1194\alpha_C - 1546 \quad (7)$$

https://doi.org/10.5194/bg-2020-410
Preprint. Discussion started: 13 November 2020

Biogeosciences Discussions Open Access EGU

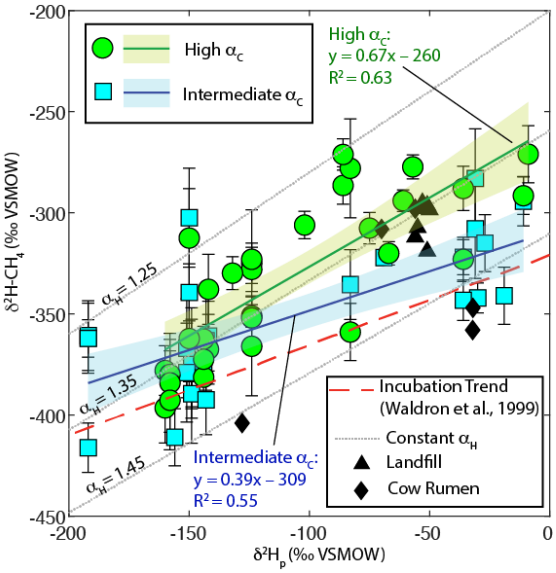

Figure 6: Scatter plot of δ^2H-CH$_4$ vs. δ^2H$_p$ with data disaggregated between sites with high and intermediate α_c values. Regression lines and error envelopes for these two groups are shown. Lines of constant α_H and a compiled trend from incubation experiments (Waldron et al., 1999) are shown for comparison. Available data from analyses of cow rumen and landfill gas are also shown (Supplemental Table S3; Douglas et al., 2020).

3.4 Differences in δ^2H-CH$_4$ and δ^{13}C-CH$_4$ between site categories

3.4.1 Differences by latitude

Kruskal-Wallis tests found a significant difference in the distribution of δ^2H-CH$_4$ between high-latitude sites (median: -362‰) and both low (median: -296‰) and mid-latitude sites (median: -316 ‰) (Fig. 7a). However, it did not find a significant difference in the distribution of low- and mid-latitude sites. A similar pattern was found when the data were disaggregated into wetland and inland water sites.

We also found that the distribution of δ^{13}C-CH$_4$ for low latitude sites (median: -61.3‰) was significantly higher than for high latitude sites (median –63.0‰), but that mid-latitude sites (median: -60.8‰) were not significantly different from the other two latitudinal zones. The observed difference by latitudinal zone in δ^{13}C-CH$_4$ appears to be driven primarily by latitudinal differences between inland water sites, where a similar pattern is found. In wetland sites we found no significant differences in the distribution of δ^{13}C-CH$_4$ by latitude.

Using resolved fluxes by latitudinal band from Saunois et al. (2020), as listed in Table 1, we calculated a flux-weighted δ^2H-CH$_4$ signature for freshwater environments of -307‰ (Fig. 7a). Similarly, we calculated a flux-weighted freshwater δ^{13}C-CH$_4$ signature of -61.5‰ (Fig. 7b).

https://doi.org/10.5194/bg-2020-410
Preprint. Discussion started: 13 November 2020

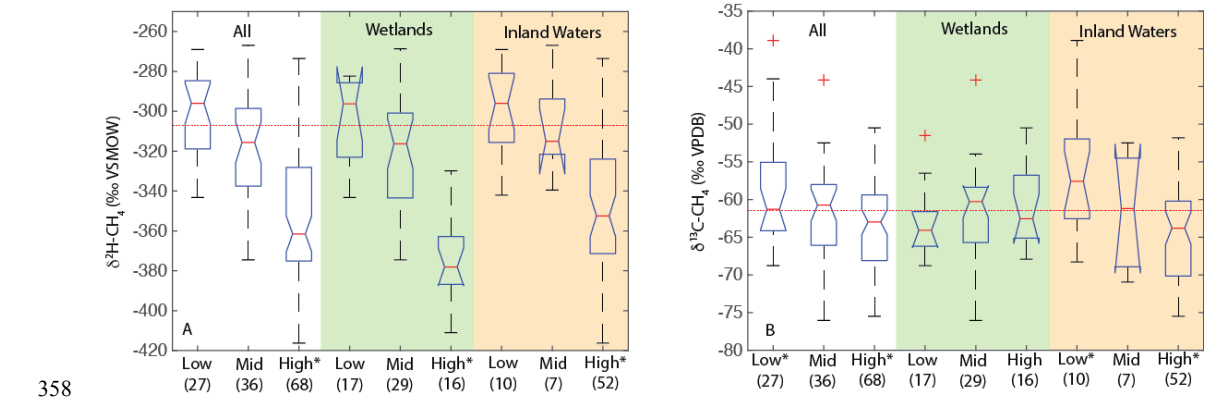

Figure 7: Boxplots of (A) δ^2H-CH_4 and (B) δ^{13}C-CH_4 for sites differentiated by latitude, for all data, wetlands, and inland waters. Numbers in parentheses indicate the number of sites for each category. Red lines indicate medians, boxes indicate 25th and 75th percentiles, whiskers indicate 95th and 5th percentiles, and outliers are shown as red crosses. Notches indicate the 95% confidence intervals of the median value; where notches overlap the edges of the box this indicates the confidence interval exceeds the 75th or 25th percentile. Red dashed lines indicate the estimated flux-weighted medians for global freshwater CH_4, as described in Sect. 3.4.1. Asterisks in (A) indicate that high-latitude sites have significantly different distributions from other latitudinal bands. Asterisks in (B) indicate groups that have significantly different distributions from one another, within a specific environmental category. One extremely high outlier (-171‰, low latitude inland water) is not shown in (A). Two extremely low outliers (<-84‰; high latitude wetland and inland water) are not shown in (B).

3.4.2 Differences by ecosystem

When comparing ecosystems, we analyze δ^2H-$CH_{4,W0}$ values to account for variability related to differences in δ^2H-H_2O. Ecosystem types are not evenly distributed by latitude, and therefore have different distributions of δ^2H-H_2O values. There are differences in the median values by ecosystem, with rivers (-296‰), bogs (-292‰), and swamps/marshes (-290‰) exhibiting relatively enriched median δ^2H-$CH_{4,W0}$, and fens (-309‰) and rice paddies (-310‰) exhibiting relatively low median values. However, given the small sample sizes and large variance in most of these categories, these differences in distributions are not significant based on a Kruskal-Wallis test. Comparing the broader categories of inland waters and wetlands with a Mann-Whitney U-test we do find a significant difference, with inland waters showing a more enriched distribution (median: -295‰) than wetlands (median: -307‰).

Similarly, we did not observe any significant differences in δ^{13}C-CH_4 values between wetland ecosystems in this dataset based on a Kruskal-Wallis test, nor between inland waters and wetlands based on a U-test. However, a U-test did indicate a significantly more enriched δ^{13}C-CH_4 distribution in rivers (median: -60.1‰) relative to lakes (median: -62.7‰).

https://doi.org/10.5194/bg-2020-410
Preprint. Discussion started: 13 November 2020

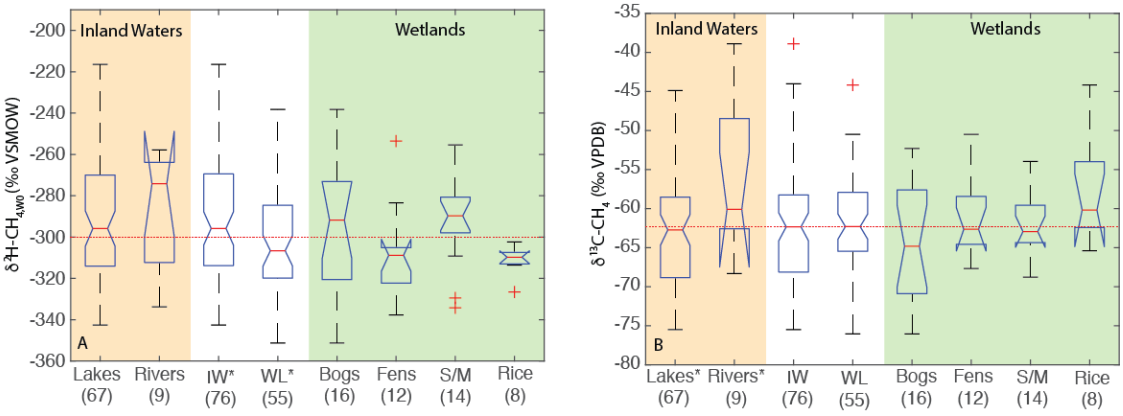

Figure 8: Boxplots of (A) δ^2H-$CH_{4,w0}$ and (B) δ^{13}C-CH_4 for sites differentiated by ecosystem type. Boxplots parameters are as in Fig. 7. Red dashed lines indicate the median values for all sites. One extremely high outlier (-160‰, river) is not shown in (A). Two extremely low outliers (<-84‰; lake and fen) are not shown in (B). IW- Inland Waters; WL- Wetlands; S/M- Swamps and marshes.

3.4.3 Differences by sample type

As with comparing ecosystems, when comparing sample types we analyze δ^2H-$CH_{4,W0}$ values to normalize for variability related to differences in δ^2H-H_2O, since sample types are not distributed evenly by latitude. When comparing sample types, dissolved CH_4 samples do not have a significantly different δ^2H-$CH_{4,W0}$ distribution for the dataset as a whole, nor is there a significant difference between these groups in wetland sites (Fig. 9). There is, however, a significant difference in inland water sites, with dissolved CH_4 samples having a more enriched distribution (median: -267‰) vs. gas samples (median: -299‰)

We did not observe a significant difference in the distribution of δ^{13}C between dissolved and gas-phase CH_4 samples, either for the dataset as a whole or when the dataset was disaggregated into wetlands and inland waters.

3.5 Estimates of global emissions source δ^2H-CH_4 and δ^{13}C-CH_4

Our mixing model and Monte Carlo analyses estimate a global source δ^2H-CH_4 of -277±8‰, and a global source δ^{13}C-CH_4 of -56.4±1.4‰ (Fig. 10). Monte Carlo sensitivity tests suggest that greater uncertainty is associated with isotopic source signatures (6‰ for δ^2H; 1.2‰ for δ^{13}C) than with flux estimates (4‰ for δ^2H; 0.7‰ for δ^{13}C).

https://doi.org/10.5194/bg-2020-410
Preprint. Discussion started: 13 November 2020

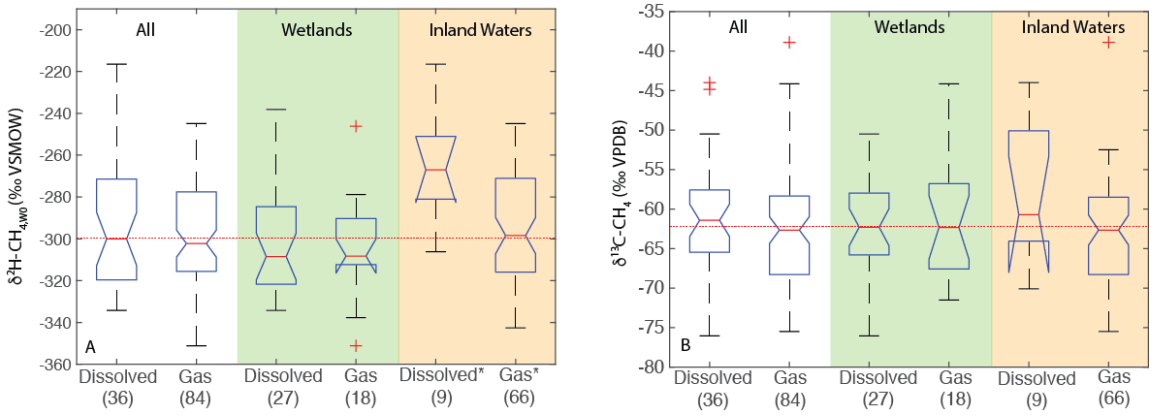

401

402 **Figure 9: Boxplots of (A) δ^2H-$CH_{4,w0}$ and (B) δ^{13}C-CH_4 for sites differentiated by sample type. Boxplots parameters are as in Fig.**
403 **7. Red dashed lines indicate the median values for all sites. One extremely high outlier (-160‰, gas inland water) is not shown in**
404 **(A). Two extremely low outliers (<-84‰; dissolved wetland and gas inland water) are not shown in (B).**

405

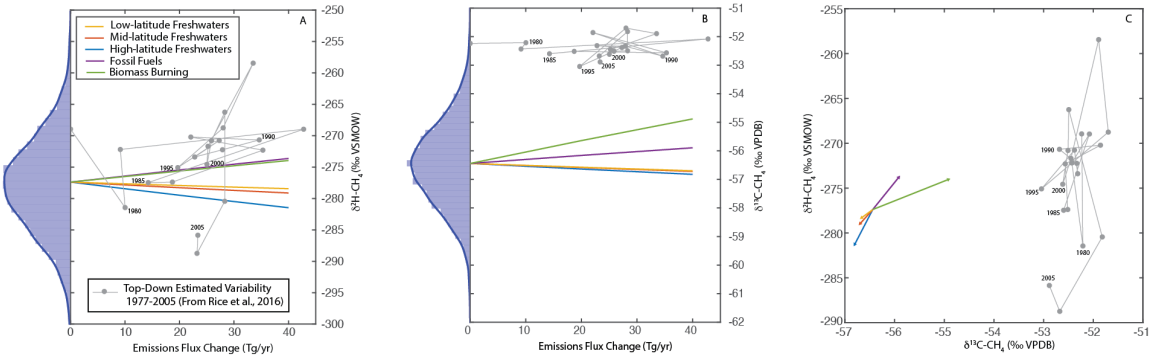

406

407 **Figure 10: Bottom-up estimates of global source δ^2H-CH_4 (A), δ^{13}C-CH_4 (B), and dual isotope signatures (C). Histograms in (A)**
408 **and (B) show probability distributions from Monte-Carlo analyses. Colored lines indicate estimated isotopic trends for increasing**
409 **emissions from specific sources, with all other emissions sources remaining constant. Colored vectors in (C) indicate the dual-**
410 **isotope trend for increasing emissions fluxes from specific sources by 40 Tg/yr, with all other emissions sources remaining**
411 **constant. Gray lines and points indicate top-down estimates of emissions source isotopic signatures from 1977 to 2005 (Rice et al.,**
412 **2016). Selected individual years are indicated. In (A) and (B) top-down flux change estimates were normalized to the first year of**
413 **the time series (1977) to facilitate comparison with the bottom-up estimates.**

https://doi.org/10.5194/bg-2020-410
Preprint. Discussion started: 13 November 2020

Our calculations imply that changes in high-latitude freshwater CH_4 emissions fluxes have a larger effect on global source δ^2H-CH_4 (-0.1‰/Tg/yr) than changes in mid-latitude (-0.04‰/Tg/yr) and low-latitude (-0.03‰/Tg/yr) CH_4 emissions (Fig. 10a). There are smaller differences in the effects of increasing emissions from different latitudes on δ^{13}C values, with -0.01‰/Tg/yr for high-latitude emissions, -.007‰/Tg/yr for mid-latitude emissions, and -.006‰/Tg/yr for low-latitude emissions (Fig. 10b). These trends lead to different slopes in a δ^2H vs. δ^{13}C bi-plot for increased freshwater emissions from these latitudinal bands (Fig. 10C): -11 for increasing high-latitude emissions, -6 for increasing mid-latitude emissions, and -4 for increasing low-latitude emissions. Increasing fossil fuel emissions results in a slope of +7, and increasing biomass burning emissions results in a slope of +2.

4 Discussion

4.1 The global dependence of δ^2H-CH_4 on δ^2H-H_2O

Our analysis confirms, using an expanded dataset, previous inferences that δ^2H-H_2O is an important predictor of global freshwater δ^2H-CH_4 (Waldron et al., 1999b; Whiticar, 1999; Chanton et al., 2006). In this study we found that modeled δ^2H_p is roughly as strong of a predictor of δ^2H-CH_4 as δ^2H-H_2O_m (Fig. 3A). This implies that isotope-enabled Earth Systems models (ESMs) could be used to predict the distribution of freshwater δ^2H-CH_4 under past and future climates. The southern hemisphere remains highly underrepresented in available δ^2H-CH_4 data. However, the mechanisms linking δ^2H-CH_4 with H_2O-δ^2H should not differ significantly in the southern hemisphere, and we argue that the relationships observed in this study are suitable to predict southern hemisphere freshwater δ^2H-CH_4.

Our analysis found an overall weaker and flatter regression relationship between these variables than the most recent comprehensive analysis of this topic (Waldron et al., 1999). This difference is probably partially the result of the much larger proportion of inland water sites (58%) in our dataset versus that of Waldron (25%). Bottom-up emissions estimates for the period 2000-2009 implied that inland waters represent 48% of total freshwater emissions (Saunois et al., 2020), although this proportion is highly uncertain. As shown in Fig. 3b, inland water sites have a lower slope for δ^2H-CH_4 vs. δ^2H_p than wetland sites, and the wetland specific regression relationship is more similar to the relationship reported by Waldron et al. (1999). However, even our wetland regression relationship has a flatter slope than reported in Waldron et al. (1999).

The different regression relationships by environment type imply that understanding the relative balance of emissions from wetlands and inland waters could be important in accurately estimating global freshwater δ^2H-CH_4. The difference in δ^2H-CH_4 between these environments is especially pronounced at high latitudes. A logical next step in predicting global freshwater δ^2H-CH_4 source signatures would be to combine high-resolution mapping of wetlands and inland waters, maps of

https://doi.org/10.5194/bg-2020-410
Preprint. Discussion started: 13 November 2020

the global distribution of δ^2H_p, and regression relationships between δ^2H-CH_4 vs. δ^2H_p. When applying such an approach it may be prudent to use the environment specific regression relationships shown in Fig. 3b.

4.2 Latitudinal differences in δ^2H-CH_4

The dependence of δ^2H-CH_4 on δ^2H_p translates directly into latitudinal variation in δ^2H-CH_4 (Fig. 4), and our results indicate that there are significant differences in the distribution of freshwater δ^2H-CH_4 values between high-latitude sites and mid- and low-latitude sites (Fig. 7A). The mean δ^2H-CH_4 for mid-latitude sites is ^2H-depleted relative to low-latitude sites, but we cannot confirm they form different distributions. It is noteworthy that based on our analysis high-latitude sites can be distinguished from both mid- and low-latitude sites, given that the northern mid-latitudes are estimated to represent a relatively large fraction of total natural CH_4 emissions based on bottom-up estimates (~30%; Saunois et al., 2020).

Latitudinal differentiation of δ^2H-CH_4 has the potential to aid in geographic discrimination of freshwater methane sources, both because it is based on a clear mechanistic linkage with δ^2H-H_2O, and because geographic variation in δ^2H-H_2O is well understood. However, recent studies of atmospheric δ^2H-CH_4 variation have not accounted for geographic variation in source signals. As an example, Rice et al., (2016) apply a constant δ^2H-CH_4 of -322‰ for both low-latitude (0-30º N) and high latitude (30- 90º N) wetland emissions. Based on our dataset this estimate is an inaccurate representation of freshwater δ^2H-CH_4 for either 0-30º N (median: -296‰) or 30-90º N (median: -340‰), and is substantially lower than our global flux-weighted mean δ^2H-CH_4 for freshwater environments (-307‰). Studies of ice core data have more frequently applied different freshwater δ^2H-CH_4 values as a function of latitude. For example, Bock et al., (2010) differentiated δ^2H-CH_4 between tropical (-320‰) and boreal (-370‰) wetlands. These values are lower than our estimates for freshwater environments on the whole (Fig. 7a), although the boreal wetland estimate of Bock et al., (2010) is similar to our median value for high-latitude wetlands (-378‰). Overall, our results imply that accounting for latitudinal variation in freshwater δ^2H-CH_4, along with latitudinal flux estimates, is important for developing accurate estimates of global δ^2H-CH_4 source signatures.

4.2.1 Comparison with latitudinal differences in $\delta^{13}C$-CH_4

Our analysis indicates significant differences in the distribution of freshwater $\delta^{13}C$-CH_4 between the low- and high-latitudes, but mid-latitude sites cannot be differentiated. Furthermore our results do not indicate significant latitudinal differences in $\delta^{13}C$-CH_4 for wetland sites in particular, whereas we do observe significant differences between the low- and high-latitudes for inland water sites. This is in contrast to previous studies that have inferred significant differences in wetland $\delta^{13}C$-CH_4 by latitude (Ganesan et al., 2018; Bock et al., 2010; Rice et al., 2016). An important caveat is that we have not analyzed a comprehensive dataset of freshwater $\delta^{13}C$-CH_4, for which there is much more published data than for δ^2H-CH_4, although to our knowledge this is the largest compiled dataset of freshwater $\delta^{13}C$-CH_4 to date. In addition, we do not take into account

https://doi.org/10.5194/bg-2020-410
Preprint. Discussion started: 13 November 2020

the geographic distribution of different ecosystem types, although our analysis also does not find significant differences in $\delta^{13}C\text{-}CH_4$ between ecosystem types (Fig. 8; Sect. 3.4.2; Sect. 4.4). Latitudinal differences in $\delta^{13}C\text{-}CH_4$ inferred by Ganesan et al. (2018) were based on two key mechanisms: (1) differences in methanogenic pathway between different types of wetlands, especially between minerotrophic fens and ombrotrophic bogs; and (2) differential inputs of organic carbon from C_3 and C_4 plants. Because inferred latitudinal differences in $\delta^{13}C\text{-}CH_4$ and $\delta^{2}H\text{-}CH_4$ are caused by different mechanisms, they could be highly complementary in validating estimates of freshwater emissions by latitude. It is also important to note that previous assessments of latitudinal differences in $\delta^{13}C\text{-}CH_4$ have not included inland water environments. A benefit of geographic discrimination based on $\delta^{2}H\text{-}CH_4$ is that the same causal mechanism applies to total freshwater emissions, including both wetlands and inland waters.

4.2.2 Potential for geographic discrimination of other microbial methane sources

We speculate that latitudinal differences in $\delta^{2}H\text{-}CH_4$ should also be observed in other fluxes of microbial methane from terrestrial environments, including enteric fermentation in livestock and wild animals, manure ponds, landfills, and termites. This is because microbial methanogenesis in all of these environments will incorporate hydrogen from environmental water, and therefore will be influenced by variation in precipitation $\delta^{2}H$. There is limited data currently available to test this prediction, but $\delta^{2}H\text{-}CH_4$ data from cow rumen and landfills that are available with either specified locations or $\delta^{2}H\text{-}H_2O$ (Liptay et al., 1998; Levin et al., 1993; Teasdale et al., 2019; Bilek et al., 2001; Wang et al., 2015; Burke, 1993) plot in a range that is consistent with the $\delta^{2}H\text{-}CH_4$ vs. $\delta^{2}H\text{-}H_2O$ relationships for freshwater CH_4 (Fig. 6). Landfill data are only available for a very small range of $\delta^{2}H_p$, making it impossible to assess for geographic variation, but the available data plot in a range spanning our regression relationships for inferred hydrogenotrophic and acetoclastic methanogenesis. $\delta^{2}H\text{-}CH_4$ data from cow rumen span a much wider range, and express substantial variation that is independent of $\delta^{2}H\text{-}H_2O$. However, the cow rumen data do imply hydrogen isotope apparent fractionation that is similar to the range observed in freshwater environments. Based on these limited data, we suggest that both landfill and cow rumen $\delta^{2}H\text{-}CH_4$ likely vary geographically as a function of $\delta^{2}H\text{-}H_2O$, and that this variation could be used to distinguish these CH_4 sources geographically, although they are likely to be substantially influenced by other variables as well. More data is clearly needed to test this conjecture, and it will also be important to evaluate how closely $\delta^{2}H_p$ corresponds to environmental $\delta^{2}H\text{-}H_2O$ in both landfills and cow rumen.

4.3 Influence of methanogenic pathways and methane oxidation on $\delta^{2}H\text{-}CH_4$

The observed co-variation between $\delta^{2}H\text{-}CH_{4,W0}$ and α_C (Fig. 5b) is consistent with previous inferences that methanogenic pathways and methane oxidation have a significant effect on freshwater $\delta^{2}H\text{-}CH_4$ (Chanton et al., 2006; Whiticar, 1999). Our analysis implies that methane oxidation in particular can have a large effect on $\delta^{2}H\text{-}CH_4$ in freshwater environments,

https://doi.org/10.5194/bg-2020-410
Preprint. Discussion started: 13 November 2020


Biogeosciences Discussions Open Access EGU

503 corresponding to variability on the order of 130‰. However, we note that of the 66 sites with $\delta^{13}C\text{-}CO_2$ data, only 6 had
504 $\delta^{2}H\text{-}CH_4$ values that were evidently influenced by methane oxidation (Fig. 5b). Of these, four sites were from the Amazon
505 River (Lansdown, 1994). Inferred $\delta^{2}H\text{-}CH_4$ variability related to differing methanogenic pathways is also pronounced, on the
506 order of 60‰. This source of variation influences a much larger proportion of the sites in our dataset, making up 90% of
507 sites with $\delta^{13}C\text{-}CO_2$ measurements. Multivariate regression suggests that, when sites with apparent methane oxidation are
508 excluded, 65% of variability in $\delta^{2}H\text{-}CH_4$ can be explained jointly by $\delta^{2}H\text{-}H_2O$ and α_C. This multivariate relationship could
509 potentially be used to improve spatial predictions of $\delta^{2}H\text{-}CH_4$, although geographic variation in α_C is not well defined.
510 It is important to note that other biogeochemical variables have the potential to influence both α_C and $CH_4\text{-}\delta^{2}H$, and
511 could be partly responsible for the variation observed in Fig. 5b. In particular, some studies have suggested that α_H varies as
512 a function of the reversibility of methanogenesis (Valentine et al., 2004b; Stolper et al., 2015), which potentially scales with
513 rates of methane production. The influence of the reversibility of methanogenesis on α_H is supported by a correlation
514 between this variable and measurements of multiply substituted, or clumped, isotopologues of CH_4, which are also predicted
515 to vary as a function of methanogenesis reversibility (Stolper et al., 2015; Douglas et al., 2017; Douglas et al., 2016).
516 Enzymatic reversibility of methanogenesis has also been inferred to influence α_C (Valentine et al., 2004b; Penning et al.,
517 2005), although the relative importance of this mechanism versus methanogenic pathway in natural environments remains
518 unclear.
519 It is intriguing that $\delta^{13}C\text{-}CO_2$ also exhibits a piece-wise linear relationship with $\delta^{2}H\text{-}CH_{4,W0}$ (Fig. 5c), which is
520 consistent with the predicted influence of methane oxidation and methanogenic pathways, but that $\delta^{13}C\text{-}CH_4$ does not (Fig.
521 5a). This is unexpected, both because $\delta^{13}C\text{-}CH_4$ is typically thought to be significantly influenced by both methane oxidation
522 and methanogenic pathways (Whiticar, 1999), and because in freshwater environments it is probable that a wide range of
523 biotic and abiotic processes unrelated to methane cycling influence $\delta^{13}C\text{-}CO_2$. Our observations are partially explained by
524 the greater overlap in the predicted fields for methanogenic pathway dependent variability and methane-oxidation dependent
525 variability in the plot of $\delta^{13}C\text{-}CH_4$ vs. $\delta^{2}H\text{-}CH_{4,W0}$ (Fig. 5a) than $\delta^{13}C\text{-}CO_2$ vs. $\delta^{2}H\text{-}CH_{4,W0}$ (Fig. 5c). Second, we speculate
526 that variability in organic matter $\delta^{13}C$ could be an important factor influencing $\delta^{13}C\text{-}CH_4$ that does not affect $\delta^{2}H\text{-}CH_{4,W0}$.
527 This has been previously inferred in terms of $\delta^{13}C$ differences between wetlands dominated by C_3 vs. C_4 plants (Ganesan et
528 al., 2018). It could also be important in inland water environments, where sedimentary organic matter can vary widely in
529 $\delta^{13}C$ (Conrad et al., 2011), in part as a function of the relative abundance of terrigenous and autochthonous organic matter
530 (France, 1995). Third, given the large difference in $\delta^{13}C$ between CO_2 and CH_4, even small changes in CO_2 concentrations
531 resulting from hydrogenotrophic methanogenesis or CH_4 oxidation can have a disproportionate isotopic fractionation on
532 $\delta^{13}C\text{-}CO_2$. While not definitive, our results are consistent with other studies implying that there are complications in using
533 $\delta^{13}C\text{-}CH_4$ as an unambiguous proxy for methanogenic pathway (Penning et al., 2005; Penning et al., 2006; Conrad et al.,
534 2011). We argue that, where possible, combined measurements of $\delta^{13}C\text{-}CH_4$, $\delta^{13}C\text{-}CO_2$, $\delta^{2}H\text{-}CH_4$, and $\delta^{2}H\text{-}H_2O$ will provide

https://doi.org/10.5194/bg-2020-410
Preprint. Discussion started: 13 November 2020

535 the greatest specificity in identifying methanogenic pathways and the extent of methane oxidation within a specific
536 environment.

537 **4.3.1 Influence of methanogenic pathway on the δ^2H-CH_4 vs. δ^2H-H_2O relationship**

538 Our results imply a difference in the δ^2H-CH_4 vs. δ^2H-H_2O relationship for samples with high α_C values and intermediate α_C
539 values (Fig. 6). This is consistent with predicted differences in this relationship between hydrogenotrophic methanogenesis
540 (high α_C) and acetoclastic methanogenesis (intermediate α_C) (Chanton et al., 2006;Whiticar, 1999). Previous research
541 predicted that hydrogenotrophic methanogenesis should express a δ^2H-CH_4 vs. δ^2H-H_2O slope of 1 (Whiticar, 1999), but
542 constant hydrogen isotope fractionation between H_2O and CH_4 would result in a flatter slope, ranging from 0.8 to 0.69 for α_H
543 values between 1.25 and 1.45 (Fig. 6). The regression relationship for sites with high α_C (hydrogenotrophic methanogenesis)
544 is consistent with the slope and intercept for α_H of 1.35. It is likely that α_H for hydrogenotrophic methanogenesis in fact
545 varies widely in natural environments (Chanton et al., 2006; Douglas et al., 2016; Douglas et al., 2017), but this agreement
546 suggests that 1.35 could be a representative mean α_H for this process in freshwater ecosystems.
547 The intermediate α_C (acetoclastic methanogenesis) regression relationship has a much flatter slope (0.39±.13) that is
548 not consistent with a constant α_H value (Fig. 6). The slope of this relationship is within error of the slope for methanogenesis
549 incubation experiments reported by Waldron et al. (1999b) (0.44±0.03), although the intercept is higher (-309‰ vs. -321‰).
550 We argue that this agreement implies that the incubation experiment regression relationship is a good approximation for the
551 δ^2H-CH_4 vs. δ^2H-H_2O relationship in natural environments dominated by acetoclastic methanogenesis.
552 Previous work predicted a slope of 0.25 for acetoclastic methanogenesis (Whiticar, 1999), and pure culture experiments have
553 also found a relatively flat slope of approximately 0.15 (Gruen et al., 2018). However, this prediction does not take into
554 account that the δ^2H of acetate methyl hydrogen is probably also influenced by environmental δ^2H-H_2O, and therefore likely
555 varies geographically as a function of δ^2H_p. To our knowledge there are no measurements of acetate or acetate-methyl δ^2H
556 from natural environments with which to test this idea. In general, variability in the δ^2H of environmental organic molecules,
557 including fatty acids and cellulose, is largely controlled by δ^2H-H_2O (Huang et al., 2002;Sachse et al., 2012;Mora and
558 Zanazzi, 2017), albeit with widely varying fractionation factors. We argue therefore that the δ^2H of acetate derived from
559 fermentation would be partly controlled by environmental δ^2H-H_2O. Furthermore, culture experiments with acetogenic
560 bacteria imply that there is rapid isotopic exchange between H_2 and H_2O during chemoautotrophic acetogenesis (Valentine et
561 al., 2004a), implying that the δ^2H of chemoautotrophic acetate is also influenced by environmental δ^2H-H_2O. Incubation
562 experiments, such as those synthesized by Waldron et al. (1999b), are likely to contain acetate δ^2H that is partially controlled
563 by ambient δ^2H-H_2O, given that the acetate inthese incubation experiments was probably actively produced by fermentation
564 and/or acetogenesis during the course of the experiment. This differs from pure cultures of methanogens, where acetate is

https://doi.org/10.5194/bg-2020-410
Preprint. Discussion started: 13 November 2020


Biogeosciences Discussions Open Access EGU

565 provided in the culture medium and therefore would not vary in its δ^2H value, unless this was explicitly controlled in the
566 experiment.

567 **4.4 Isotopic differences in CH_4 between ecosystems**

568 The absence of significant differences in $\delta^2H\text{-}CH_{4,W0}$ distributions between specific ecosystem types could be the result of
569 small samples sizes for most ecosystems. We do observe large apparent differences in median $\delta^2H\text{-}CH_{4,W0}$ between some
570 ecosystem categories (Fig. 8a), and further studies could be targeted towards verifying these differences. Specifically, rice
571 paddies and fens have low median $\delta^2H\text{-}CH_{4,W0}$, which could reflect a greater proportion of acetoclastic methanogenesis in
572 these ecosystems (Ganesan et al., 2018; Hornibrook, 2009; Conrad and Klose, 1999). In contrast, relatively high median
573 $\delta^2H\text{-}CH_{4,W0}$ for bogs and marshes/swamps could be related to a greater degree of hydrogenotrophic methanogenesis in these
574 environments (Ganesan et al., 2018; Hornibrook, 2009). However, bogs especially express a very high degree of variability
575 in $\delta^2H\text{-}CH_{4,W0}$, suggesting that methanogenic pathways may be highly variable between different bogs, as has been
576 previously inferred in studies of $\delta^{13}C\text{-}CH_4$ (Hornibrook, 2009). High median values in river ecosystems, in contrast, are
577 likely a function of greater rates of oxidation, given that these environments are also characterized by relatively high $\delta^{13}C\text{-}$
578 CH_4 (Fig. 8b). As noted above (Sect. 4.3), these sites also tend to have low values for α_c. We suggest that greater oxidation in
579 fluvial environments could be a result of reduced stratification compared to other inland water environments, and therefore
580 greater dissolved oxygen and potential for aerobic oxidation in the water column and sediments. However, our river dataset
581 is highly biased towards the Amazon river basin, and drawing firm conclusions will require a larger and more widely
582 distributed dataset. There is a significant difference in the distribution of $\delta^2H\text{-}CH_{4,W0}$ between the broader categories of
583 inland waters and wetlands. This difference is primarily a result of the difference in $\delta^2H\text{-}CH_4$ between these environments in
584 the high latitudes (Fig. 3b). We are unsure of the mechanism causing this difference, though it may be partly related to a
585 greater overall prevalence of CH_4 oxidation in inland waters, as discussed above and in Sect. 4.5.

586 In our dataset differences in $\delta^{13}C\text{-}CH_4$ distributions between ecosystem types are also generally not significant, and
587 are less pronounced than for $\delta^2H\text{-}CH_{4,W0}$ (Fig. 8b). The one exception to this is significantly higher $\delta^{13}C\text{-}CH_4$ in rivers
588 relative to lakes, which is consistent with greater CH_4 oxidation in rivers. Among wetlands, rice paddies have somewhat
589 higher median $\delta^{13}C\text{-}CH_4$, and bogs have somewhat lower median $\delta^{13}C\text{-}CH_4$, but the uncertainty in these median values
590 overlaps the median for the dataset as a whole. This is in contrast to previous studies that have suggested that fens and bogs
591 in particular have distinctive $\delta^{13}C\text{-}CH_4$ (Ganesan et al., 2018). As noted above, this result should be interpreted with caution
592 given that our dataset is not a comprehensive compilation of published $\delta^{13}C\text{-}CH_4$ data. However, we argue that differences in
593 $\delta^{13}C\text{-}CH_4$ between wetland ecosystem categories require further verification before being inferred confidently.
594
595

https://doi.org/10.5194/bg-2020-410
Preprint. Discussion started: 13 November 2020

596 **4.5 Isotopic differences between dissolved and gas-phase CH_4**

597 In general we do not observe significant, or even apparent, differences in CH_4 isotopic composition between sites where
598 dissolved and gas-phase samples were analyzed. The one exception to this is high $\delta^2H\text{-}CH_{4,W0}$ in dissolved samples relative
599 to gas samples from inland water environments. We suggest this could be a result of generally greater oxidation of dissolved
600 CH_4 in inland water environments, potentially as a result of longer exposure to aerobic conditions in lake or river water
601 columns. This is in contrast to wetlands, where aerobic conditions are generally limited to the uppermost layers of wetlands
602 proximate to the water table. However, our dataset for inland water dissolved CH_4 is quite small (n=9), and more data is
603 needed to test this hypothesis. No difference between dissolved and gas-phase samples are clearly apparent for $\delta^{13}C$, either
604 for inland waters or wetlands.
605 Overall, our data imply that isotopic differences between dissolved and gas phase methane are relatively minor on a
606 global basis, and therefore that the relative balance of diffusive vs. ebullition gas fluxes should not have a large effect on the
607 isotopic composition of freshwater CH_4 emissions. However, our study does not specifically account for isotopic
608 fractionation occurring during diffusive or plant-mediated transport (Hornibrook, 2009), and most of our dissolved sample
609 data are of *in-situ* dissolved CH_4 and not diffusive fluxes. More isotopic data specifically focused on diffusive methane
610 emissions, for example using measurements of gas sampled from chambers, would help to resolve this question.

611 **4.6 Implications for atmospheric CH_4 isotopic composition**

612 Our bottom-up estimate of global atmospheric source $\delta^2H\text{-}CH_4$, -277±8‰, is within the range of top-down estimates from
613 1977-2005 (-258 to -289‰) (Rice et al., 2016). In contrast our estimate is significantly higher than a previous bottom-up
614 estimate of modern global atmospheric source $\delta^2H\text{-}CH_4$ (-295‰) (Whiticar and Schaefer, 2007). We suggest this difference
615 is due to the use of much more depleted $\delta^2H\text{-}CH_4$ source signatures for tropical and boreal wetlands by Whiticar and
616 Schaefer (2007).
617 Our bottom-up estimate of global atmospheric source $\delta^{13}C\text{-}CH_4$ (-56.4±1.4‰) is significantly lower than the range
618 of top-down estimates from 1977-2005 (-51.7 to -53‰) (Rice et al., 2016). This discrepancy in $\delta^{13}C\text{-}CH_4$ estimates could be
619 the result of one or more of the following: (1) errors in the sink fluxes or fractionation factors applied by Rice et al. (2016);
620 (2) biases in our applied $\delta^{13}C\text{-}CH_4$ source signatures towards $\delta^{13}C$ enriched values; or (3) biases in the bottom-up flux
621 estimates of Saunois et al. (2020) towards ^{13}C enriched sources. Our estimate is also more depleted than the modern bottom-
622 up estimate of Whiticar and Schaefer (2007), -54.2‰.
623 One plausible bias in our source signatures is that we have not included high $\delta^{13}C\text{-}CH_4$ values from tropical
624 wetlands dominated by C_4 plants (Ganesan et al., 2018). However our global flux weighted $\delta^{13}C\text{-}CH_4$ for freshwater
625 environments (-61.5‰) is higher than that of Ganesan et al. (2018), -62‰. Furthermore, changing the tropical wetland $\delta^{13}C$-

https://doi.org/10.5194/bg-2020-410
Preprint. Discussion started: 13 November 2020

626 CH_4 signature source signature in our mixing model to the average tropical signature inferred by Ganesan et al. (2018) (-
627 56.7‰) only increases our estimated global $\delta^{13}C$-CH_4 to -55.1±1.4‰, which is still inconsistent with top-down estimates.
628 Another plausible cause of the observed discrepancy between bottom-up and top-down $\delta^{13}C$-CH_4 estimates is that
629 emissions inventories underestimate fossil-fuel emissions and overestimate microbial emissions (Schwietzke et al., 2016).
630 We examined this scenario by increasing fossil fuel emissions in our mixing model by a factor of two, and decreased all
631 microbial sources by a factor of two. In this scenario bottom-up $\delta^{13}C$-CH_4 is -52±1.6‰, which is within the range of top-
632 down estimates. However, this also results in a much greater bottom-up $\delta^{2}H$-CH_4 of -250±9‰, which is not consistent with
633 most top-down estimates from 1977-2005 (Fig. 10).
634 A final scenario that could potentially reconcile bottom-up and top-down estimates of both $\delta^{13}C$-CH_4 and $\delta^{2}H$-CH_4
635 is a large increase in biomass burning emissions (Fig. 10C). We examined this scenario by increasing biomass burning
636 emissions by a factor of 4, and decreasing all other emissions sources by 10%. This results in $\delta^{13}C$-CH_4 of -52.8±1.64‰ and
637 $\delta^{2}H$-CH_4 of -269±7‰, which are both consistent with the range of top-down estimates. However, we are uncertain whether
638 such a large increase of biomass burning emissions is plausible.
639 Another interesting result of comparing our bottom-up estimates with top-down estimates from 1977-2005 is that
640 the top-down estimates, taken at face value, imply very large changes in global source $\delta^{2}H$-CH_4 on interannual timescales.
641 As shown in Fig. 10A, these changes generally have a steep positive slope in terms of $\delta^{2}H$-CH_4 vs. changes in CH_4 flux. This
642 suggests that inter-annual variability during this period was primarily driven by changes in fossil fuel or biomass burning
643 emissions. However, the slopes of interannual variability shown in in Fig. 10A are too steep to be caused by changes in these
644 emissions sources alone. We suggest they require either (1) concomitant changes in microbial sources of an opposite sign
645 (e.g. an increase in fossil fuel emissions combined with a decrease in freshwater emissions); or (2) changes in the sink fluxes
646 or isotopic fractionations that are not accounted for in the model of Rice et al. (2016). In contrast the trend towards lower
647 $\delta^{2}H$-CH_4 between 2002-2005 likely involved an increase in microbial emissions, but based on the trends shown in Fig. 10A
648 would have required concomitant reductions in fossil fuel or biomass burning emissions.
649 Ultimately, fully accounting for variability in atmospheric $\delta^{2}H$-CH_4 is beyond the scope of this paper and will
650 require more in-depth models of source and sink processes. However, based on the analysis above, we argue that the large
651 variability in atmospheric $\delta^{2}H$-CH_4 is an important constraint on global CH_4 budgets that has been under-utilized, but that
652 has strong potential to complement $\delta^{13}C$-CH_4 measurements and modeling. This is especially true now that advances in
653 measurement technology are making an expansion of both atmospheric and source $\delta^{2}H$-CH_4 measurements increasingly
654 practical (Chen et al., 2016; Röckmann et al., 2016; Yacovitch et al., 2020). Based on our dataset and analysis, atmospheric
655 $\delta^{2}H$-CH_4 measurements could be especially valuable in identifying increasing high-latitude freshwater CH_4 emissions
656 resulting from permafrost thaw (Koven et al., 2011).

https://doi.org/10.5194/bg-2020-410
Preprint. Discussion started: 13 November 2020


Biogeosciences Discussions Open Access EGU

5 Conclusions

Our analysis of an expanded isotopic dataset for freshwater CH_4 confirms previous assertions that $\delta^2H\text{-}H_2O$ is a primary determinant of $\delta^2H\text{-}CH_4$ on a global scale (Whiticar, 1999; Chanton et al., 2006; Waldron et al., 1999b), but also finds that the slope of this relationship is flatter than was inferred in previous studies (Fig. 3a). This flatter slope may be the result of the inclusion of a greater proportion of inland water sites in our dataset. Our analysis also indicates that modeled δ^2H_p is a good proxy for the effects of $\delta^2H\text{-}H_2O$ on $\delta^2H\text{-}CH_4$, implying that isotope-enabled climate models could be used to predict the distribution of $\delta^2H\text{-}CH_4$ in past and future climates. We find that residual variability in $\delta^2H\text{-}CH_4$ is related to variance in methanogenic pathway and CH_4 oxidation, as reflected by α_c values (Fig. 5b). In contrast, $\delta^{13}C\text{-}CH_4$ is not a significant predictor of $\delta^2H\text{-}CH_4$ variability (Fig. 5a). Together $\delta^2H\text{-}H_2O$ and α_c account for about 67% of variability in $\delta^2H\text{-}CH_4$, when excluding sites with inferred methane oxidation. By using α_c to classify sites on the basis of the dominant methanogenic pathway, we find that sites dominated by hydrogenotrophic methanogenesis express a relatively steep $\delta^2H\text{-}H_2O$ vs. $\delta^2H\text{-}CH_4$ slope that is consistent with a constant α_H value of approximately 1.35 (Fig. 6). In contrast, sites dominated by acetoclastic methanogenesis express a flatter $\delta^2H\text{-}H_2O$ vs. $\delta^2H\text{-}CH_4$ slope that is not consistent with a uniform α_H value, but is similar to the slope observed in incubation experiments (Waldron et al., 1999b).

The dependence of $\delta^2H\text{-}CH_4$ on $\delta^2H\text{-}H_2O$ leads to clear latitudinal differences in $\delta^2H\text{-}CH_4$, with particularly low values from high latitude sites (Fig. 7a). This implies that atmospheric $\delta^2H\text{-}CH_4$ could be a valuable tracer for the geographic distribution of freshwater CH_4 emissions, and potentially other microbial CH_4 sources as well. The mechanism for latitudinal differences in $\delta^2H\text{-}CH_4$ is distinct from proposed mechanisms for latitudinal differences in $\delta^{13}C\text{-}CH_4$ (Ganesan et al., 2018), implying that these two isotopic tracers are complementary in validating geographic emissions sources. Atmospheric $\delta^2H\text{-}CH_4$ is especially sensitive to changes in high-latitude freshwater emissions, and could be valuable in constraining future methane emissions from thawing permafrost (Fig. 10A). We estimate a global flux-weighted $\delta^2H\text{-}CH_4$ signature from freshwater environments of -307‰, which is significantly enriched relative to values used in previous source apportionment studies (Rice et al., 2016; Bock et al., 2017). Even when the effects of $\delta^2H\text{-}H_2O$ are accounted for we do not observe significant differences in $\delta^2H\text{-}CH_4$ between ecosystem types or sample types (Fig. 8 and 9), with the exception of higher values in dissolved samples relative to gas samples in inland water environments. However, there are apparent differences between some wetland ecosystems that could be verified with larger datasets.

Our bottom-up estimate of the global $\delta^2H\text{-}CH_4$ source signature, -277±8‰, is consistent with top-down estimates based on atmospheric measurements between 1977 and 2005 (Rice et al., 2016), but our bottom-up estimate of global $\delta^{13}C\text{-}CH_4$, -56.4±1.4‰, is not consistent with these top-down estimates. We suggest that this discrepancy is likely the result of either (1) error in estimated sink fluxes or fractionations; or (2) a bias in inventory estimates towards microbial CH_4 sources. Increased biomass burning emissions is one scenario that could reconcile bottom-up and top-down emissions estimates in terms of both $\delta^{13}C\text{-}CH_4$ and $\delta^2H\text{-}CH_4$. During the 1977-2005 period there were large interannual changes in estimated source

https://doi.org/10.5194/bg-2020-410
Preprint. Discussion started: 13 November 2020

689 δ^2H-CH_4 that cannot be accounted for by changes in a single source term alone. In general, the large variability observed in
690 atmospheric δ^2H-CH_4, combined with its distinctive source and sink signatures and new measurement technologies, suggest
691 this measurement has strong potential as a tool to help resolve atmospheric methane budgets.
692
693 **Data Availability:** The datasets used in this paper (Supplementary Tables 1-3) are publicly available: Douglas, Peter;
694 Stratigopoulos, Emerald; Park, Jenny; Phan, Dawson (2020): Data for geographic variability in freshwater methane
695 hydrogen isotope ratios and its implications for emissions source apportionment and microbial biogeochemistry. figshare.
696 Dataset. https://doi.org/10.6084/m9.figshare.13194833.v1
697
698 **Author Contribution:** PMJD designed the project, assisted with compiling the data, analyzed the data, and wrote the
699 manuscript; ES and JP compiled the data, and assisted with analyzing the data and editing the manuscript; DP developed
700 code for mixing model and Monte Carlo calculations, and assisted with analyzing the data and editing the manuscript.
701
702 **Competing Interests:** The authors declare they have no competing interests.
703
704 **Acknowledgments:** We thank all of the researchers whose published data made this analysis possible (See Supplemental
705 Table 1). This research was partially funded by McGill Science Undergraduate Research Awards to ES and JP and by
706 NSERC Discovery Grant 2017-03902 to PMJD.

707 **References**

708 Alstad, K. P., and Whiticar, M. J.: Carbon and hydrogen isotope ratio characterization of methane dynamics for Fluxnet
709 Peatland Ecosystems, Org Geochem, 42, 548-558, 2011.
710 Bailer, A. J.: Statistics for environmental biology and toxicology, Routledge, 2020.
711 Bastviken, D., Tranvik, L. J., Downing, J. A., Crill, P. M., and Enrich-Prast, A.: Freshwater methane emissions offset the
712 continental carbon sink, Science, 331, 50-50, 2011.
713 Bellisario, L., Bubier, J., Moore, T., and Chanton, J.: Controls on CH4 emissions from a northern peatland, Global
714 Biogeochem Cy, 13, 81-91, 1999.
715 Bergamaschi, P.: Seasonal variations of stable hydrogen and carbon isotope ratios in methane from a Chinese rice paddy,
716 Journal of Geophysical Research: Atmospheres, 102, 25383-25393, 1997.
717 Bilek, R., Tyler, S., Kurihara, M., and Yagi, K.: Investigation of cattle methane production and emission over a 24-hour
718 period using measurements of δ13C and δD of emitted CH4 and rumen water, Journal of Geophysical Research:
719 Atmospheres, 106, 15405-15413, 2001.

https://doi.org/10.5194/bg-2020-410
Preprint. Discussion started: 13 November 2020

720 Bock, M., Schmitt, J., Möller, L., Spahni, R., Blunier, T., and Fischer, H.: Hydrogen isotopes preclude marine hydrate CH4
721 emissions at the onset of Dansgaard-Oeschger events, Science, 328, 1686-1689, 2010.
722 Bock, M., Schmitt, J., Beck, J., Seth, B., Chappellaz, J., and Fischer, H.: Glacial/interglacial wetland, biomass burning, and
723 geologic methane emissions constrained by dual stable isotopic CH4 ice core records, Proceedings of the National Academy
724 of Sciences, 114, E5778-E5786, 2017.
725 Bouchard, F., Laurion, I., Preskienis, V., Fortier, D., Xu, X., and Whiticar, M.: Modern to millennium-old greenhouse gases
726 emitted from ponds and lakes of the Eastern Canadian Arctic (Bylot Island, Nunavut), Biogeosciences, 12, 7279-7298, 2015.
727 Bowen, G. J., and Wilkinson, B.: Spatial distribution of δ18O in meteoric precipitation, Geology, 30, 315-318, 2002.
728 Bowen, G. J., and Revenaugh, J.: Interpolating the isotopic composition of modern meteoric precipitation, Water Resources
729 Research, 39, -, Artn 1299
730 Doi 10.1029/2003wr002086, 2003.
731 Bowen, G. J., Wassenaar, L. I., and Hobson, K. A.: Global application of stable hydrogen and oxygen isotopes to wildlife
732 forensics, Oecologia, 143, 337-348, 2005.
733 Brosius, L., Walter Anthony, K., Grosse, G., Chanton, J., Farquharson, L., Overduin, P. P., and Meyer, H.: Using the
734 deuterium isotope composition of permafrost meltwater to constrain thermokarst lake contributions to atmospheric CH4
735 during the last deglaciation, Journal of Geophysical Research: Biogeosciences (2005–2012), 117, 2012.
736 Burke Jr, R.: SHALLOW AQUATIC SEDIMENTS, Bacterial Gas. Conference, Mila, September 25-26, 1989, 1992, 47,
737 Burke Jr, R. A., and Sackett, W. M.: Stable hydrogen and carbon isotopic compositions of biogenic methanes from several
738 shallow aquatic environments, in, ACS Publications, 1986.
739 Burke Jr, R. A., Barber, T. R., and Sackett, W. M.: Methane flux and stable hydrogen and carbon isotope composition of
740 sedimentary methane from the Florida Everglades, Global Biogeochem Cy, 2, 329-340, 1988.
741 Burke Jr, R. A., Barber, T. R., and Sackett, W. M.: Seasonal variations of stable hydrogen and carbon isotope ratios of
742 methane in subtropical freshwater sediments, Global Biogeochem Cy, 6, 125-138, 1992.
743 Burke Jr, R. A.: Possible influence of hydrogen concentration on microbial methane stable hydrogen isotopic composition,
744 Chemosphere, 26, 55-67, 1993.
745 Cadieux, S. B., White, J. R., Sauer, P. E., Peng, Y., Goldman, A. E., and Pratt, L. M.: Large fractionations of C and H
746 isotopes related to methane oxidation in Arctic lakes, Geochim Cosmochim Ac, 187, 141-155, 2016.
747 Chanton, J., Whiting, G., Blair, N., Lindau, C., and Bollich, P.: Methane emission from rice: Stable isotopes, diurnal
748 variations, and CO2 exchange, Global Biogeochem Cy, 11, 15-27, 1997.
749 Chanton, J. P., Fields, D., and Hines, M. E.: Controls on the hydrogen isotopic composition of biogenic methane from high-
750 latitude terrestrial wetlands, Journal of Geophysical Research: Biogeosciences (2005–2012), 111, 2006.
751 Chasar, L., Chanton, J., Glaser, P. H., and Siegel, D.: Methane concentration and stable isotope distribution as evidence of
752 rhizospheric processes: Comparison of a fen and bog in the Glacial Lake Agassiz Peatland complex, Annals of Botany, 86,
753 655-663, 2000.

https://doi.org/10.5194/bg-2020-410
Preprint. Discussion started: 13 November 2020

754 Chen, Y., Lehmann, K. K., Peng, Y., Pratt, L., White, J., Cadieux, S., Sherwood Lollar, B., Lacrampe-Couloume, G., and
755 Onstott, T. C.: Hydrogen Isotopic Composition of Arctic and Atmospheric CH4 Determined by a Portable Near-Infrared
756 Cavity Ring-Down Spectrometer with a Cryogenic Pre-Concentrator, Astrobiology, 16, 787-797, 2016.
757 Clay, A., Bradley, C., Gerrard, A., and Leng, M.: Using stable isotopes of water to infer wetland hydrological dynamics,
758 Hydrology and Earth System Sciences, 8, 1164-1173, 2004.
759 Conrad, R., and Klose, M.: How specific is the inhibition by methyl fluoride of acetoclastic methanogenesis in anoxic rice
760 field soil?, FEMS Microbiology Ecology, 30, 47-56, 1999.
761 Conrad, R., Noll, M., Claus, P., Klose, M., Bastos, W., and Enrich-Prast, A.: Stable carbon isotope discrimination and
762 microbiology of methane formation in tropical anoxic lake sediments, Biogeosciences, 8, 795, 2011.
763 Douglas, P.M.J., Stolper, D., Smith, D., Walter Anthony, K., Paull, C., Dallimore, S., Wik, M., Crill, P., Winterdahl, M.,
764 Eiler, J., and Sessions, A. L.: Diverse origins of Arctic and Subarctic methane point source emissions identified with
765 multiply-substituted isotopologues, Geochim Cosmochim Ac, 188, 163-188, 2016.
766 Douglas, P. M.J., Stolper, D. A., Eiler, J. M., Sessions, A. L., Lawson, M., Shuai, Y., Bishop, A., Podlaha, O. G., Ferreira, A.
767 A., and Neto, E. V. S.: Methane clumped isotopes: progress and potential for a new isotopic tracer, Org Geochem, 113, 262-
768 282, 2017.
769 Douglas, P.M.J. Stratigopoulos, E., Park, J., and Phan, D. (2020): Data for geographic variability in freshwater methane
770 hydrogen isotope ratios and its implications for emissions source apportionment and microbial biogeochemistry. figshare.
771 Dataset. https://doi.org/10.6084/m9.figshare.13194833.v1
772 Drevon, D., Fursa, S. R., and Malcolm, A. L.: Intercoder reliability and validity of WebPlotDigitizer in extracting graphed
773 data, Behavior modification, 41, 323-339, 2017.
774 Dunn, O. J.: Multiple comparisons using rank sums, Technometrics, 6, 241-252, 1964.
775 France, R. L.: Differentiation between littoral and pelagic food webs in lakes using stable carbon isotopes, Limnol Oceanogr,
776 40, 1310-1313, 1995.
777 Ganesan, A., Stell, A., Gedney, N., Comyn-Platt, E., Hayman, G., Rigby, M., Poulter, B., and Hornibrook, E.: Spatially
778 resolved isotopic source signatures of wetland methane emissions, Geophys Res Lett, 45, 3737-3745, 2018.
779 Gruen, D. S., Wang, D. T., Könneke, M., Topçuoğlu, B. D., Stewart, L. C., Goldhammer, T., Holden, J. F., Hinrichs, K.-U.,
780 and Ono, S.: Experimental investigation on the controls of clumped isotopologue and hydrogen isotope ratios in microbial
781 methane, Geochim Cosmochim Ac, 237, 339-356, 2018.
782 Happell, J. D., Chanton, J. P., Whiting, G. J., and Showers, W. J.: Stable isotopes as tracers of methane dynamics in
783 Everglades marshes with and without active populations of methane oxidizing bacteria, Journal of Geophysical Research:
784 Atmospheres, 98, 14771-14782, 1993.
785 Happell, J. D., Chanton, J. P., and Showers, W. S.: The influence of methane oxidation on the stable isotopic composition of
786 methane emitted from Florida swamp forests, Geochim Cosmochim Ac, 58, 4377-4388, 1994.

https://doi.org/10.5194/bg-2020-410
Preprint. Discussion started: 13 November 2020

787 Hornibrook, E. R., Longstaffe, F. J., and Fyfe, W. S.: Spatial distribution of microbial methane production pathways in
788 temperate zone wetland soils: stable carbon and hydrogen isotope evidence, Geochim Cosmochim Ac, 61, 745-753, 1997.
789 Hornibrook, E. R.: The stable carbon isotope composition of methane produced and emitted from northern peatlands, Baird,
790 A., Belyea, L., Comas, X., Reeve, A., and Slater, L., American Geophysical Union, Geophysical Monograph Series, 184,
791 187-203, 2009.
792 Huang, Y., Shuman, B., Wang, Y., and Webb III, T.: Hydrogen isotope ratios of palmitic acid in lacustrine sediments record
793 late Quaternary climate variations, Geology, 30, 1103-1106, 2002.
794 Kai, F. M., Tyler, S. C., Randerson, J. T., and Blake, D. R.: Reduced methane growth rate explained by decreased Northern
795 Hemisphere microbial sources, Nature, 476, 194-197, 2011.
796 Koven, C. D., Ringeval, B., Friedlingstein, P., Ciais, P., Cadule, P., Khvorostyanov, D., Krinner, G., and Tarnocai, C.:
797 Permafrost carbon-climate feedbacks accelerate global warming, Proceedings of the National Academy of Sciences, 108,
798 14769-14774, 2011.
799 Kruskal, W. H., and Wallis, W. A.: Use of ranks in one-criterion variance analysis, Journal of the American statistical
800 Association, 47, 583-621, 1952.
801 Lansdown, J., Quay, P., and King, S.: CH4 production via CO2 reduction in a temperate bog: A source of 13C-depIeted
802 CH4, Geochim Cosmochim Ac, 56, 3493-3503, 1992.
803 Lansdown, J. M.: The carbon and hydrogen stable isotope composition of methane released from natural wetlands and
804 ruminants, 1994.
805 Lecher, A. L., Chuang, P. C., Singleton, M., and Paytan, A.: Sources of methane to an Arctic lake in Alaska: An isotopic
806 investigation, Journal of Geophysical Research: Biogeosciences, 122, 753-766, 2017.
807 Levin, I., Bergamaschi, P., Dörr, H., and Trapp, D.: Stable isotopic signature of methane from major sources in Germany,
808 Chemosphere, 26, 161-177, 1993.
809 Liptay, K., Chanton, J., Czepiel, P., and Mosher, B.: Use of stable isotopes to determine methane oxidation in landfill cover
810 soils, Journal of Geophysical Research: Atmospheres, 103, 8243-8250, 1998.
811 Mann, H. B., and Whitney, D. R.: On a test of whether one of two random variables is stochastically larger than the other,
812 The annals of mathematical statistics, 50-60, 1947.
813 Marik, T., Fischer, H., Conen, F., and Smith, K.: Seasonal variations in stable carbon and hydrogen isotope ratios in methane
814 from rice fields, Global Biogeochem Cy, 16, 41-41-41-11, 2002.
815 Martens, C. S., Kelley, C. A., Chanton, J. P., and Showers, W. J.: Carbon and hydrogen isotopic characterization of methane
816 from wetlands and lakes of the Yukon-Kuskokwim delta, western Alaska, Journal of Geophysical Research: Atmospheres
817 (1984–2012), 97, 16689-16701, 1992.
818 Mischler, J. A., Sowers, T. A., Alley, R. B., Battle, M., McConnell, J., Mitchell, L., Popp, T., Sofen, E., and Spencer, M.:
819 Carbon and hydrogen isotopic composition of methane over the last 1000 years, Global Biogeochem Cy, 23, 2009.

https://doi.org/10.5194/bg-2020-410
Preprint. Discussion started: 13 November 2020

820 Mora, G., and Zanazzi, A.: Hydrogen isotope ratios of moss cellulose and source water in wetlands of Lake Superior, United
821 States reveal their potential for quantitative paleoclimatic reconstructions, Chem Geol, 468, 75-83, 2017.
822 Nakagawa, F., Yoshida, N., Nojiri, Y., and Makarov, V.: Production of methane from alasses in eastern Siberia: Implications
823 from its 14C and stable isotopic compositions, Global Biogeochem Cy, 16, 14-11-14-15, 2002a.
824 Nakagawa, F., Yoshida, N., Sugimoto, A., Wada, E., Yoshioka, T., Ueda, S., and Vijarnsorn, P.: Stable isotope and
825 radiocarbon compositions of methane emitted from tropical rice paddies and swamps in Southern Thailand,
826 Biogeochemistry, 61, 1-19, 2002b.
827 Penning, H., Plugge, C. M., Galand, P. E., and Conrad, R.: Variation of carbon isotope fractionation in hydrogenotrophic
828 methanogenic microbial cultures and environmental samples at different energy status, Global Change Biol, 11, 2103-2113,
829 2005.
830 Penning, H., Claus, P., Casper, P., and Conrad, R.: Carbon isotope fractionation during acetoclastic methanogenesis by
831 Methanosaeta concilii in culture and a lake sediment, Applied and Environmental Microbiology, 72, 5648-5652, 2006.
832 Pison, I., Ringeval, B., Bousquet, P., Prigent, C., and Papa, F.: Stable atmospheric methane in the 2000s: key-role of
833 emissions from natural wetlands, 2013.
834 Polissar, P. J., and D'Andrea, W. J.: Uncertainty in Paleohydrologic Reconstructions from Molecular δD Values, Geochim
835 Cosmochim Ac, 2013.
836 Popp, T. J., Chanton, J. P., Whiting, G. J., and Grant, N.: Methane stable isotope distribution at a Carex dominated fen in
837 north central Alberta, Global Biogeochem Cy, 13, 1063-1077, 1999.
838 Rice, A. L., Butenhoff, C. L., Teama, D. G., Röger, F. H., Khalil, M. A. K., and Rasmussen, R. A.: Atmospheric methane
839 isotopic record favors fossil sources flat in 1980s and 1990s with recent increase, Proceedings of the National Academy of
840 Sciences, 113, 10791-10796, 2016.
841 Röckmann, T., Eyer, S., Van Der Veen, C., Popa, M. E., Tuzson, B., Monteil, G., Houweling, S., Harris, E., Brunner, D., and
842 Fischer, H.: In situ observations of the isotopic composition of methane at the Cabauw tall tower site, Atmos. Chem. Phys.,
843 16, 10469-10487, 2016.
844 Rozanski, K., Araguás-Araguás, L., and Gonfiantini, R.: Isotopic patterns in modern global precipitation, Geophysical
845 Monograph Series, 78, 1-36, 1993.
846 Sachse, D., Billault, I., Bowen, G. J., Chikaraishi, Y., Dawson, T. E., Feakins, S. J., Freeman, K. H., Magill, C. R.,
847 McInerney, F. A., and van der Meer, M. T. J.: Molecular paleohydrology: Interpreting the hydrogen-isotopic composition of
848 lipid biomarkers from photosynthesizing organisms, Annual Review of Earth and Planetary Sciences, 40, 221-249, 2012.
849 Sakagami, H., Takahashi, N., Hachikubo, A., Minami, H., Yamashita, S., Shoji, H., Khlystov, O., Kalmychkov, G., Grachev,
850 M., and De Batist, M.: Molecular and isotopic composition of hydrate-bound and dissolved gases in the southern basin of
851 Lake Baikal, based on an improved headspace gas method, Geo-Mar Lett, 32, 465-472, 2012.
852 Saunois, M., Stavert, A. R., Poulter, B., Bousquet, P., Canadell, J., Jackson, R. B., Raymond, P. A., and Dlugokencky, E.:
853 The global methane budget 2000–2017, Earth System Science Data, 2019.

https://doi.org/10.5194/bg-2020-410
Preprint. Discussion started: 13 November 2020

854 Saunois, M., Stavert, A. R., Poulter, B., Bousquet, P., Canadell, J. G., Jackson, R. B., Raymond, P. A., Dlugokencky, E. J.,
855 Houweling, S., and Patra, P. K.: The global methane budget 2000–2017, Earth System Science Data, 12, 1561-1623, 2020.
856 Schaefer, H., Fletcher, S. E. M., Veidt, C., Lassey, K. R., Brailsford, G. W., Bromley, T. M., Dlugokencky, E. J., Michel, S.
857 E., Miller, J. B., and Levin, I.: A 21st-century shift from fossil-fuel to biogenic methane emissions indicated by 13CH4,
858 Science, 352, 80-84, 2016.
859 Schoell, M.: Genetic characterization of natural gases, AAPG bulletin, 67, 2225-2238, 1983.
860 Schwietzke, S., Sherwood, O. A., Bruhwiler, L. M., Miller, J. B., Etiope, G., Dlugokencky, E. J., Michel, S. E., Arling, V.
861 A., Vaughn, B. H., and White, J. W.: Upward revision of global fossil fuel methane emissions based on isotope database,
862 Nature, 538, 88-91, 2016.
863 Shapiro, S. S., and Wilk, M. B.: An analysis of variance test for normality (complete samples), Biometrika, 52, 591-611,
864 1965.
865 Sherwood, O. A., Schwietzke, S., Arling, V. A., and Etiope, G.: Global inventory of gas geochemistry data from fossil fuel,
866 microbial and burning sources, version 2017, Earth System Science Data, 9, 2017.
867 Stolper, D., Martini, A., Clog, M., Douglas, P., Shusta, S., Valentine, D., Sessions, A., and Eiler, J.: Distinguishing and
868 understanding thermogenic and biogenic sources of methane using multiply substituted isotopologues, Geochim Cosmochim
869 Ac, 161, 219-247, 2015.
870 Teasdale, C. J., Hall, J. A., Martin, J. P., and Manning, D. A.: Discriminating methane sources in ground gas emissions in
871 NW England, Quarterly Journal of Engineering Geology and Hydrogeology, 52, 110-122, 2019.
872 Thompson, H. A., White, J. R., Pratt, L. M., and Sauer, P. E.: Spatial variation in flux, δ 13 C and δ 2 H of methane in a
873 small Arctic lake with fringing wetland in western Greenland, Biogeochemistry, 131, 17-33, 2016.
874 Thompson, K. M., Burmaster, D. E., and Crouch3, E. A.: Monte Carlo techniques for quantitative uncertainty analysis in
875 public health risk assessments, Risk Analysis, 12, 53-63, 1992.
876 Townsend-Small, A., Botner, E. C., Jimenez, K. L., Schroeder, J. R., Blake, N. J., Meinardi, S., Blake, D. R., Sive, B. C.,
877 Bon, D., and Crawford, J. H.: Using stable isotopes of hydrogen to quantify biogenic and thermogenic atmospheric methane
878 sources: A case study from the Colorado Front Range, Geophys Res Lett, 43, 11,462-411,471, 2016.
879 Turner, A. J., Frankenberg, C., and Kort, E. A.: Interpreting contemporary trends in atmospheric methane, Proceedings of the
880 National Academy of Sciences, 116, 2805-2813, 2019.
881 Tyler, S., Bilek, R., Sass, R., and Fisher, F.: Methane oxidation and pathways of production in a Texas paddy field deduced
882 from measurements of flux, δl3C, and δD of CH4, Global Biogeochem Cy, 11, 323-348, 1997.
883 Valentine, D., Sessions, A., Tyler, S., and Chidthaisong, A.: Hydrogen isotope fractionation during H2/CO2 acetogenesis:
884 hydrogen utilization efficiency and the origin of lipid-bound hydrogen, Geobiology, 2, 179-188, 2004a.
885 Valentine, D. L., Chidthaisong, A., Rice, A., Reeburgh, W. S., and Tyler, S. C.: Carbon and hydrogen isotope fractionation
886 by moderately thermophilic methanogens, Geochim Cosmochim Ac, 68, 1571-1590, 2004b.

https://doi.org/10.5194/bg-2020-410
Preprint. Discussion started: 13 November 2020

887 Wahlen, M.: Carbon dioxide, carbon monoxide and methane in the atmosphere: abundance and isotopic composition, Stable
888 isotopes in ecology and environmental science, 93-113, 1994.
889 Waldron, S., Hall, A. J., and Fallick, A. E.: Enigmatic stable isotope dynamics of deep peat methane, Global Biogeochem
890 Cy, 13, 93-100, 1999a.
891 Waldron, S., Lansdown, J., Scott, E., Fallick, A., and Hall, A.: The global influence of the hydrogen iostope composition of
892 water on that of bacteriogenic methane from shallow freshwater environments, Geochim Cosmochim Ac, 63, 2237-2245,
893 1999b.
894 Walter, K., Chanton, J. P., Chapin, F. S., Schuur, E. A. G., and Zimov, S. A.: Methane production and bubble emissions
895 from arctic lakes: Isotopic implications for source pathways and ages, J Geophys Res-Biogeo, 113, Artn G00a08
896 Doi 10.1029/2007jg000569, 2008.
897 Walter, K. M., Zimov, S., Chanton, J. P., Verbyla, D., and Chapin, F. S.: Methane bubbling from Siberian thaw lakes as a
898 positive feedback to climate warming, Nature, 443, 71-75, 2006.
899 Wang, D. T., Gruen, D. S., Sherwood Lollar, B., Hinrichs, K.-U., Stewart, L. C., Holden, J. F., Hristov, A. N., Pohlman, J.
900 W., Morrill, P. L., Könneke, M., Delwiche, K. B., Reeves, E. P., Sutcliffe, C. N., Ritter, D. J., Seewald, J. S., McIntosh, J.
901 C., Hemond, H. F., Kubo, M. D., Cardace, D., Hoehler, T. M., and Ono, S.: Nonequilibrium clumped isotope signals in
902 microbial methane, Science, 348, 428-431, 2015.
903 Wassmann, R., Thein, U., Whiticar, M., Rennenburg, H., Seiler, W., and Junk, W.: Methane emissions from the Amazon
904 floodplain: characterization of production and transport, Global Biogeochem Cy, 6, 3-13, 1992.
905 Whiticar, M., and Schaefer, H.: Constraining past global tropospheric methane budgets with carbon and hydrogen isotope
906 ratios in ice, Philosophical Transactions of the Royal Society A: Mathematical, Physical and Engineering Sciences, 365,
907 1793-1828, 2007.
908 Whiticar, M. J., Faber, E., and Schoell, M.: Biogenic methane formation in marine and freshwater environments: CO_2
909 reduction *vs.* acetate fermentation—Isotope evidence, Geochim Cosmochim Ac, 50, 693-709, 1986.
910 Whiticar, M. J.: Carbon and hydrogen isotope systematics of bacterial formation and oxidation of methane, Chem Geol, 161,
911 291-314, 1999.
912 Woltemate, I., Whiticar, M., and Schoell, M.: Carbon and hydrogen isotopic composition of bacterial methane in a shallow
913 freshwater lake, Limnol Oceanogr, 29, 985-992, 1984.
914 Yacovitch, T. I., Daube, C., and Herndon, S. C.: Methane emissions from offshore oil and gas platforms in the Gulf of
915 Mexico, Environmental Science & Technology, 54, 3530-3538, 2020.
916 Yvon-Durocher, G., Allen, A. P., Bastviken, D., Conrad, R., Gudasz, C., St-Pierre, A., Thanh-Duc, N., and Del Giorgio, P.
917 A.: Methane fluxes show consistent temperature dependence across microbial to ecosystem scales, Nature, 507, 488-491,
918 2014.

https://doi.org/10.5194/bg-2020-410
Preprint. Discussion started: 13 November 2020

919 Zhang, Z., Zimmermann, N. E., Stenke, A., Li, X., Hodson, E. L., Zhu, G., Huang, C., and Poulter, B.: Emerging role of
920 wetland methane emissions in driving 21st century climate change, Proceedings of the National Academy of Sciences, 114,
921 9647-9652, 2017.
922 Zhu, J., Liu, Z., Brady, E., Otto-Bliesner, B., Zhang, J., Noone, D., Tomas, R., Nusbaumer, J., Wong, T., and Jahn, A.:
923 Reduced ENSO variability at the LGM revealed by an isotope-enabled Earth system model, Geophys Res Lett, 44, 6984-
924 6992, 2017.
925 Zimov, S., Voropaev, Y. V., Semiletov, I., Davidov, S., Prosiannikov, S., Chapin, F. S., Chapin, M., Trumbore, S., and
926 Tyler, S.: North Siberian lakes: a methane source fueled by Pleistocene carbon, Science, 277, 800-802, 1997.
927